SCHOLARLY REVIEW

ISSUE#3

Fall 2022

contact@scholarlyreview.org

About

The Scholarly Review is an open-access, quarterly journal dedicated to publishing academic research in the natural sciences, social sciences and humanities. Our independent editorial board is made of highly accomplished professors and academics in corresponding fields who review student submissions and select pieces for publication.

Editorial Board

European University, Budapest and completing postgraduate specialization at NIOD Institute for War, Holocaust and Genocide Studies in Amsterdam. He has published extensively on foreign policy of socialist Yugoslavia and on the history of ethnic cleansing (Etničko čišćenje: geneza koncepta, Arhipelag, 2019). His latest book in English, The Emergence of Historical Forensic Expertise: Clio takes the Stand (Routledge, 2017) examines the role of historians and social scientists as expert witnesses in some of the most dramatic legal reckonings with the violent past.

Dr. Ana-Maria Piso-Grigore is an independent scientist and researcher with over 10 years of experience in applying data science and artificial intelligence techniques to astrophysics problems. She holds two bachelor degrees in Physics and Math from M.I.T. (2010), and a Ph. D. in Astronomy and Astrophysics from Harvard University (2016). Her doctoral research has focused on theoretical studies and modeling of extrasolar planet compositions. She held two postdoctoral positions at UCLA and CSUN, where she continued my exoplanet research studying planet formation and protoplanetary disk evolution. At that time, she also became highly interested in artificial intelligence and data science, to which end she completed a 6-month internship as a data scientist at a medical device company. In 2019, she returned to her home country, Romania, where she is currently working as Project Manager and Science Data Processing Engineer at a private company in the space sector. Here, she is managing and coordinating internal activities for upgrading SST tools for optical telescopes using AI capabilities. In parallel, she is leading business development activities for science missions related advances, with the goal of developing novel tools and solutions to facilitate exoplanet data processing using AI. She has four peer-reviewed publications in the Astrophysical Journal as lead author with over 300 citations in total.

Ms. Avi-Yona Israel is an accomplished academic scholar and lawyer with a JD from University of Pennsylvania Law School, including the Exceptional Pro Bono Service Award (200+ hours). She has studied at the University of Oxford, the Wharton School at Penn, and she received her undergraduate degree from Colgate University. Among other roles she serves as a director of advocacy and mentor to dozens of young scholars.

Dr. Ganesh Mani is an adjunct faculty member at Carnegie Mellon University. Ganesh co-founded Advanced Investment Technology (combining investment management and machine learning), which was acquired by State Street Corporation, creating its Advanced Research Centre for helping manage multibillion-dollar institutional portfolios. Ganesh has contributed to other AI start-ups, including an entity that's now part of Nasdaq-listed iCAD, employing machine learning techniques for early cancer detection. Ganesh has an MBA in finance and a PhD in AI from the University of Wisconsin-Madison. He is a board member of The Indus Entrepreneurs (TiE. org), Pittsburgh chapter, and on the advisory board of the FDP Institute. Ganesh's work has been patented and featured in a Barron's cover story and in academic journals.

The editorial board also acknowledges the support of our valued student and graduate board members, including for this issue:

Minghui Zhang, who received her Bachelor of Science degree in Biotechnology from Sun Yat-sen University, Guangzhou, China, in 2020. She is currently pursuing a Master of Health Science degree in Epidemiology at Johns Hopkins Bloomberg School of Public Health. Her research interests include control and prevention of infectious disease, molecular and genetic mechanisms of disease transmission, and global health promotion.

Editorial: SR Issue 3 Oct 2022

Welcome to the 3rd issue of Scholarly Review, a multi-disciplinary journal, providing emerging scholars with a platform where they can share their work and enjoy the benefits of having an online peer-reviewed journal publication. The editors have been impressed by the high standard of submissions, and readers should expect to find stimulating essays to read on a broad range of topics. We hope that readers share our enthusiasm and enjoy the journal and that it may help to inspire future contributions from young scholars.

This issue contains eight papers. Ghosh, Zeng and Xiao discuss scientific applications of cloud technology to analyze moves within the sport of fencing to help players find optimal, winning moves. H Zhao writes about using neural networks to examine rockfall patterns on Mars and the Moon, thereby helping scientists learn more about geological formations, with the potential to increase value and efficiency for future rover missions. E He writes about traumatic brain injuries caused by high contact sport, looking at biomarkers, classifications, and the need for tighter rules to provide better levels of protection for athletes. D Hu looks for a ‘best fit model’ in theoretical physics using Chi-squared analysis to account for uncertainty in relation to ‘falling chain dynamics’.

SJ Liu addresses topical problems around environmental pollution caused by intensive farming in China; using data from the National Bureau of Statistics in China and the World Bank, the author assesses negative impacts that these methods are having on climate change. Within a context of increasingly unstable markets, C Su examines stock market variations, applying artificial intelligence and predictive algorithms to help guide amateur investors. E Sun’s paper utilizes machine learning algorithms to predict the melting points of chemical compounds, comparing Recurrent Convolutional Networks and a Simplified Molecular Input Line Entry System. Z Li assesses the legacy of Napoleonic Law and how it has perhaps been over-emphasized and afforded higher status than it deserves; taking Latin America as an example, levels of originality are evaluated in relation to precedents of relative antiquity.

Scholarly Review

TABLE OF CONTENTS

AI Fencing Recommender using Cloud Technology and IoT

By Nilansh Dey Ghosh, Oliver Zeng, and Tony Xiao

Author Bio

We are all high school students who have a common interest in computer science. Two of the three authors have past experience with fencing, which is another major theme of this paper/project. We are all located in North America, and we range from rising grade 11 to rising university students. We received guidance from Dr. Jean-Claude Franchitti from New York University.

Abstract

The purpose of our project is to use artificial intelligence to provide feedback to a fencer through a video upload. Our project will use an artificial intelligence program capable of analyzing fencers through deep learning. We will specifically be examining Sabre. The general skeleton of our system relies on using motion capture technology to input data into our AI and applying deep learning technology to analyze successful moves and those that are less successful. IoTs have already been developed that allows for whole-body motion capture, and we hope to use something similar to conduct our motion capturing. We also hope to incorporate data from a variety of sources such as youtube videos and fencing clips taken by fencers, so we will create fencer skeletons and extract motion data from such sources. We will categorize moves as strong or weak against certain people by examining the effectiveness over a certain amount of touches, and other factors such as how difficult the move itself is to do. Our theoretical program will be capable of suggesting to an athlete the most optimal moves that he/she should take to win against a certain opponent.

Keywords: Fencing, Artificial Intelligence, Sport, Cloud technology, Internet of Things, IoT, Sports Performace

Introduction

Inspiration

With artificial intelligence being incorporated into many industries, there is little surprise that the sports industry is getting involved in AI. Many popular sports have already gone through or are going through AI-influenced changes, but less popular sports such as fencing are still in the process of implementing such AIs. Our group wanted to develop such AIs because of our interest in fencing as well as AIs.

One of our sources of inspiration came from the story of how Austrian math Ph.D. and cyclist Anna Kiesenhofer achieved an Olympic gold medal. Keisenhofer was in many ways a novice at cycling compared to her competitors. However, she utilized her extensive math background to create mathematical models that helped her in training, nutrition, and game plan. She ended up having 75 second lead over the second-place cyclist, showing the world that math and science could be used to help athletes prevail.

Intrigued by her story, our group conducted further research on examples of athletes who were able to use their academic expertise to achieve athletic excellence. We found that Dick Fosbury, one of the most influential high jumpers in history, revolutionized the high jump technique back in 1968 when he was a 21-year-old novice to high jumping. Fosbury utilized his knowledge in physics to create a more optimal jumping position that manipulates his center of gravity. He would go on to achieve an Olympic gold medal and change the sport forever. His jumping technique has since become the norm for high jumpers.

From these examples, we also wanted to use our skills and background to attempt to change a sport as all our predecessors did. In the end, we have chosen fencing because many of our team members do fencing, and we will be attempting to utilize AI because we all have a programming and big data background.

Importance

Artificial intelligence with the capability to analyze other fencers could be extremely helpful in the sport of fencing. Using deep learning, we can potentially create a program that will output not only moves and strategies that fencers should choose, but also mistakes and areas of improvement that they can work on. What could be realized through years of tournaments and training can be summarized in minutes through a deep learning algorithm, and this is our ultimate goal.

There are more than 210,000 fencers in the US alone, and is a sport of growing interest. Fencing also have a very rich background and great importance, for example, fencing is one of only four sports to be debuted in every single modern Olympic. Fencing also requires a great deal of training which results in magnificent feats, such as being the second-fastest sport in the Olympic game, just behind the shooting. Fencing is also known as flexible, as its rules changed a great deal over the years to adapt better and to improve. This rich history, combined with modern technology and bonded by its flexibility will very likely result in the perfect combination.

Basic rules of Fencing:

Originally, fencing was a military practice, where two soldiers dueled each other, but during the late 14th century, fencing slowly transformed into a sport that has a huge impact on society. From the Pirates of the Caribbean to Star Trek, fencing is all there; from regional competitions to Olympic games, fencing is there; from young children to elders, fencing is played by. Despite having a huge player base, long history, and many world-class competitions, fencing is not a popular sport, but it has a very strict set of rules like all popular sports do.

There are three types of weapons in fencing, being Epee, Foil, and Saber. They are quite different from each other, but they all have some similarities. We will only discuss the very basics of fencing for if we go into too much detail, then this paper would be on the rules of fencing.

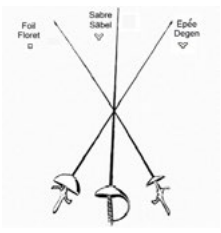

Figure 0.1 the shape of each blade

Epee is the heaviest and slowest one of the three. Historically, the epee is mainly used for dueling. Epee can hit anywhere on the body and it would count as a point. Whoever hits first will gain the point, but if both the fencers hit at the same time, then a point is awarded to both players. Epee can only register a point from compressing the tip, so the fencer must hit with the tip of the blade.

Foil is the lightest weapon, and historically, it is the practice blade for epee so it is similar to the epee. The fencer can only score on the torso of the opponent, which means there will be no point awarded if the opponent hits the mask, hand, arm, leg, and foot of the opponent. Similar to epee, a foilist also needs to hit with the tip of the blade. In foil, whoever hits first is awarded a point, but if both fencers hit at the same time, then the system of the right of the blade is in play. A player can have the right of the blade if they are attacking or is the fencer who has the intention to attack. The point will be given if the player has the right of the blade, and if both players have the right of the blade, then both players are awarded a point.

Sabre is the fastest weapon of the three and historically, the sabre is derived from cavalry fighting. The fencer can only score on the waist up, which does not include leg and foot. Sabre does not need to register a hit with the tip of the blade, as long as the blade makes contact with the target, then it is a point. Whoever hits first will be awarded the point, and if they both hit, the system of the right of blade is in play. In the sabre, the right of the blade is the same as the foil.

Figure 0.2 the red section are the target of the fencer in each sport

Related Work

Despite fencing being a less popular sport, surprisingly, it has a lot more related work than we have anticipated. There are many projects related to fencing which are ranging from extensive to just starting. We have grouped the related works into two categories, that of work related to motion capturing and the other category being the analysis of the fencing moves.

There are many projects which go into motion capturing and machine learning to assist referees. For example, Benkohn attempted to create a virtual sabre aid in which he used machine learning to break down the actions of performing sabre athletes. His project is however incomplete due to a lack of data, with only 250 available clips to use.

Another study was conducted by the Dentsu Lab of Tokyo, in which they applied motion capturing technology to highlight and track the blade movement of fencers. With more data, these results can easily be applied to a deep learning system and will make analyzing the video many times easier. The following is a summary of the route which they took.

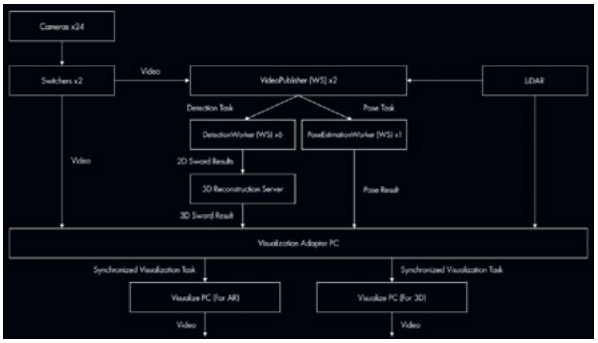

Microsoft has also created a wearable suit that allows for full-body tracking. Features such as the degrees at which the legs of a fencer are bent as well as the position of all body parts are returned as data from the suit. This suit could be combined with motion capturing data to better gather data for a deep learning program.

Jason Mo also used OpenPose, a motion tracking program to attempt to create a program that would help referees in fencing. Using OpenPose, the background and extra visual data are removed from clips of fencing, leaving only the body motion of the fencers. This could also be extremely helpful in the data gathering for our theoretical AI.

Method

Expected challenges

We suspect that tracking the blade would be difficult because the blade would be just a few pixels, making it hard for the software to track.

We suspect that tracking the blade collision would be difficult because most videos are all in 2d, which makes it extremely hard to track the collision of two objects. There are some viable solutions such as tracking the sound, creating a 3d model or putting the fencers into a controlled environment such as a recording studio. Unfortunately, all these solutions are either time-consuming or cost extensive, which we could not complete, but we will attempt to give a hypothesized solution.

We have noticed that many of the videos are different angles and qualities, so it would be hard for the software to analyze the videos.

Gather Information and Data

If we gathered the information by ourselves, it would take an enormous amount of work and time to find the large quantities of video and input them, plus the work is very repetitive. So we wanted to create a simple AI for this task. It will take less time and less work to train an actual AI than to find all the videos by ourselves.

We will train a simple AI to gather fencing videos off Youtube, the AI will do a general search and attempt to identify the targeted videos. We will train the AI in two stages. In the first stage, we will provide random fencing videos to the AI, once the AI can find a basic pattern, we will then have the AI find videos, then we will determine if the video selected is correct. Once all videos selected from the AI are correct, then the AI will be put into an unsupervised mode where it will search for videos by itself.

In addition, using IoTs such as the wearable suit designed by Microsoft could also be a source of motion capturing data. However, that technology is still in development, so we won't be considering it in our current theoretical model.

Processing Data

As mentioned, processing our data will come down to a machine learning program. This program will use motion capturing data already in development to extract important information from the clips that are inputted into the program, such as the position of the hands, legs, torso, speed, acceleration, blade movement, and blade collision. As mentioned previously, motion data of the body can easily be extracted from videos. Blade tracking, although significantly more difficult, can also be made to happen. In this scenario, we will be using a combination of the OpenPose technology that allows for body motion capturing as well as the blade tracking developed by Dentsu lab to analyze both the body and the blade. In addition, the problem of finding blade contact, which was mentioned as a challenge above, can in fact be solved by conducting 3D analysis on the 2D videos. For this, technology that allows for the reconstruction from 2D to 3D will be implemented. Using a combination of a detection server, a 3D reconstruction server and a visualization adapter, we can make this happen. This processed data will then be sent through the neural net of our program, in which scoring vs. not scoring will be analyzed. The data inputs will be as such: we will have the motion information of both fencers, inputted together as one set of data into the neural net. After creating a list of moves available, the neural net will analyze this combination of moves from opposing fencers, and strengthen a network for a set of motion data that worked well against a different set of motion data. This will be added to the list so that we will have numerical indicators of how successful a set of moves is against opposing moves. For example, a row in our data may look as such:

	Double Disengage	**Step Forward Circle Six**	**Counterattack learning forward**
Preparation on lower right blade position	1.642	2.435	4.430
Straight lunge	5.052	0.392	4.218

With each number indicating how effective the move on the horizontal was against the vertical option. The higher the number, the better the success chance. Building upon this data with consistent data additions, the program will have an accurate data value for each move and counter move.

Furthermore, deep learning can also be used to analyze and categorize fencers. For example, for each time that a fencer uses a certain move set, the neural network will up the value for this move under the fencer's name. Whether or not the move succeeds will also be collected as information. Through deep learning, the program will be able to give data of the fencer, like their likely offense and defense tactics, as well as what moves may be successful against those moves. The program would be extremely helpful in pointing out moves that usually result in the opponent losing a point.

Motion capturing can also be combined with deep learning to determine the accuracy of moves compared to what they should be when successful. For example, the program may suggest bending the legs at approximately 80 degrees when lunging for optimal success, related to speed and ability to retreat to defense. The deep learning program will analyze both moves and fencers to provide encompassing data to its users.

Analysis and Results

The goal of our model is to be able to recommend different moves and key improvements to help fencers and their coaches win matches. With video clips that can be visualized in 2D, creating an AI recommender system for fencing is challenging yet attainable. Using the work of other fencing object detectors on Github, we were able to produce an artificial intelligence model that can detect and recommend different fencing moves based on the opponent's actions. The first step in the process was to identify the fencing suit and the sabre. Creating our dataset proved to be a challenge. We converted many videos of fencing from different camera angles and lighting mechanics using OpenCV into smaller/shorter clips that were taken right before a point was scored. Having only a small video decreases the time for which the recommender will run and thus producing results more efficiently. In addition, due to sizing issues, we had to cut down on numerous clips which were either stretched or taken in portrait mode. In the end, we were able to come out with about 6,000 clips and about 12,000 after we horizontally flipped each clip to give more training to the model. Flipping the video also helps the model analyze more fencers with various playstyles. Next, we had to be able to process these video clips. Using the InceptionV3 net on each frame of a clip, we were able to take out the convolutional features (i.e converting each frame into a 1x2048 vector). That feature vector is then interpreted by one fully connected layer for the Imagenet database in the inception network, but the same feature vector should perform quite well as representations of what is going on in my frames.

Then, using the clips of these feature vectors, a multi-layer LSTM is trained. To train the model, we utilized an AWS p2 spot instance. As we don't have a lot of clips, it is more practical to utilize transfer learning to extract features rather than training my convolutional layers. Only the recurrent net on top must then learn from the ground up. I tried a few other topologies and found that 4 layers with a dropout of 0.2 work efficiently. The model begins to overfit without dropout as a regularizer. I also tested with an MNIST model which was less efficient than the LSTM.

After we were able to process the data, a recommender system was used to properly recommend different moves to the fencer and coach. In this model, we analyzed data through three types of analysis: real-time, near-real-time, and batch analysis. The next step was to filter the data to provide a realistic recommendation to the fencer in real-time. Rather than implementing content-based filtering, collaborative filtering proved to be much more effective with a memory-based filter too.

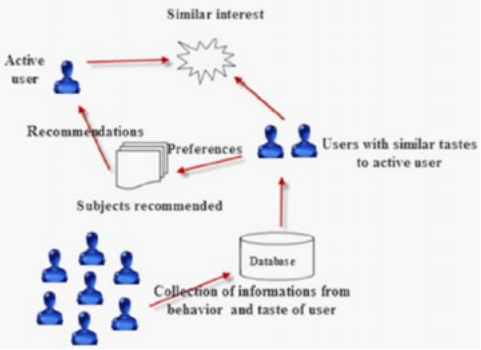

Our next step was to gain results for the model's accuracy and adjust various weights accordingly.

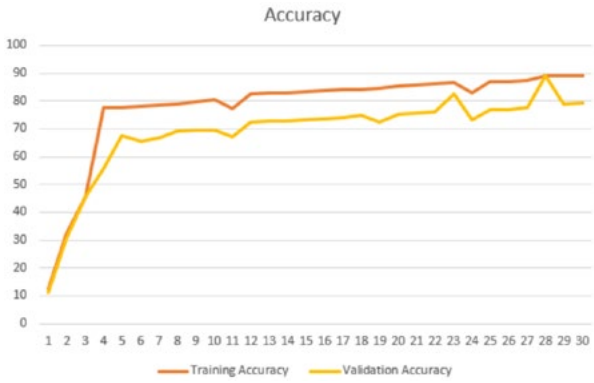

From our findings, we were able to see that the accuracy of our model was not as expected but still high enough to not be a nuisance to fencers and coaches. To further improve on the accuracy and reduction of loss, we hope to spend more time adjusting weights and possibly trying out more types of fencing moves to see if the number of inputs would change the number of outputs.

Many other fundamental aspects of our theoretical program are still in development, limiting its current application. However, following further development of motion capturing data as well as even more detailed neural networks, the program should be able to improve and eventually provide pinpoint accurate output data. What we have suggested is essentially a skeletal framework of an analytical deep learning program that can be used for many sports, and in our case fencing.

Final product

The program is open-sourced and is encouraged for all fencers to take advantage of. The link to our program will all be attached in the following google drive. Fencers and the general public is encouraged to advance the product and results from this project further.

Future challenges

- Creating motion tracking systems with better accuracy
- Extracting only necessary information from video clips, and being able to deal with low-quality clips that may be hard to work with.
- Branching further in the deep learning neural net to allow for more complex analysis such as how well a fencer is performing, whether or not they are experiencing fatigue, etc.

Conclusion

In the end, we were able to utilize artificial intelligence to provide detailed feedback to a fencer through a video upload. Our project used an artificial intelligence program capable of analyzing fencers through deep learning. For our artificial intelligence, we trained it to specifically study foil/epee. Our system relies on utilizing motion capture technology to input data into our AI and applying deep learning technology to analyze successful moves and those that are less successful in terms of probability. IoTs have already been developed that allow for whole-body motion capture, so we utilized many of the related works to aid us further. We were able to incorporate data from a variety of sources such as Youtube videos and fencing clips taken by individual fencers with consent, so we created fencer skeletons and extracted motion data from such sources. We categorized moves as strong or weak against certain people by examining the effectiveness over a certain amount of touches, and other factors such as how difficult the move itself is to do. Our program is capable of suggesting to an athlete the moves that he/she should take to win against a certain opponent.

References

1. Asia, S. (2019, October 30). *En garde! Wearable IoT and AI keep fencers on point*. Microsoft Stories Asia. https://news.microsoft.com/apac/features/en-garde-wearable-iot-and-ai-keep-fencers-on-point/

2. Benkohn. (2021, March 5). *Virtual Saber Aid*. Medium. https://medium.com/swlh/virtual-saber-aid-ece8c13b9a4d

3. Doug. (2018, June 7). *fencing-the-new-it-sport-for-kids*. Kidzu. https://kidzu.co/sports-athletics/fencing/fencing-the-new-it-sport-for-kids/

4. Malawski, F., & Kwolek, B. (2018). Recognition of action dynamics in fencing using multimodal cues. *Image and Vision Computing*, 75, 1–10. https://doi.org/10.1016/j.imavis.2018.04.005

5. Michaelsen, A. N., & Cleland, C. L. (2019). Kinematic determinants of scoring success in the fencing flick: Logistic and linear multiple regression analysis. *PLOS ONE*, 14(9), e0222075. https://doi.org/10.1371/journal.pone.0222075

6. Mo, J. (2021, August 16). *Pose Estimation and Preprocessing for an AI Fencing Referee*. Medium. https://thejasonmo.medium.com/pose-estimation-and-preprocessing-for-an-ai-fencing-referee-e63515a55dbd

7. sholtodouglas, & CodLiver, C. (2018, November 20). *GitHub - sholtodouglas/fencing-AI: Using deep learning to referee fencing*. GitHub. https://github.com/sholtodouglas/fencing-AI

8. Sugano, K., Ochi, K., Sone, R., Manabe, D., Ai, K., Ishibashi, M., & Hanai, Y. (2021, September 13). *Fencing tracking and visualization system*. Rhizomatiks. https://research.rhizomatiks.com/s/works/fencing_tracking/

9. *Sword Types*. (2009). Uni-Kiel.de. https://www.tf.uni-kiel.de/matwis/amat/iss/kap_1/basics/b1_1_3.html

The Impact of Neural Network Complexity on the Detection of Rockfalls on Mars and the Moon

By Henry Zhao

Author Bio

Henry Zhao grew up in Vancouver, and is currently a grade 11 student at Collingwood school. His favorite subjects are physics and computer science, and he plans on studying mechanical engineering and computer science in university. He is the lead coder in his school robotics club, and often assists other robotics teams with programming. In his spare time, he enjoys working on personal engineering projects, 3D modeling and rendering, origami, and drawing digital art. He is a black belt in martial arts, and has been attending since 2012. He is also actively involved with community service, and helps with tutoring for both his classmates and elementary students.

Abstract

The detection of rockfalls is important to real-time tasks on celestial objects, such as finding potentially hazardous or geologically active areas on Mars. Currently, rockfall processing is done by hand, requiring a large amount of human labor. This study intends to test the effectiveness of machine learning on the detection of rockfalls on Mars and the Moon. Specifically, this study tests the impact of neural network complexity, and thus detection time, on the precision, recall, and F1 score of detection results. 5 different convolutional neural networks were trained and tested on a dataset of Mars and moon rockfalls. It was found that Resnet50 with transfer learning performed the best, with a median detection time and recall, and high precision and F1. There also is a rough pattern corresponding longer detection times with more precision and less recall, and shorter detection time with more recall and less precision. From the data gathered, it appears that it is feasible to use machine learning to quickly and effectively detect rockfalls on Mars, for use in real-time processing and decision making.

Keywords: Machine learning, binary classification, convolutional neural networks, model complexity, rockfall detection, recall, precision, F1 score, training time, classification time

Introduction

Rockfalls are common mass-wasting processes on rocky planets and satellites. They are typically driven by geological and celestial processes, including quakes and meteoritic impacts. By finding the distribution of rockfalls on a planet or satellite, the speed of erosion and geological activity in certain areas can be determined. As well, since erosion acts on the tracks of rockfalls, the density of rockfalls can reveal information about the age and geologic activity of said areas.

Currently, the priority of rockfall studies are on Mars. Such studies could reveal the geologic status of areas on Mars, and provide risk information in the possibility that Mars becomes the next human-occupied planet in our system. The current methods for detecting and studying rockfalls requires human labor to scan through satellite images, marking out all rockfalls.

As of currently, the High Resolution Imaging Science Experiment (HiRISE) imaging system on the Mars Reconnaissance Orbiter has captured only approximately 4% of the Mars surface (Slade, 2021). However, these images have a spatial resolution of up to 0.3m/pixel, meaning the amount and scale of the images gathered are quite significant. Due to this, it takes a significant amount of human labor and time to detect all rockfalls in even a single HiRISE image. It has been previously found by Valentin Tertius Bickel that machine learning, or more specifically, Convolutional Neural Networks (CNNs) were effective in the detection of rockfalls on Mars and the moon. The results showed that CNNs were faster at detecting rockfalls than humans by an order of magnitude, while maintaining an acceptable tradeoff between recall and precision (Bickel et. al, 2020). By training a neural network to identify rockfalls, the processing time and human labor can be greatly reduced, while still resulting in similar accuracy. However, this time reduction is not quantitatively reported, and it is unknown whether it is adequate for real-time processing, which will be important for real-time rover guidance or real-time geologic analysis. Thus, it is necessary to further explore the possibility of optimizing current algorithms, to analyze the potential for processing in near-real-time situations.

The objective of this study is to determine the relationship between the recall or precision of a model compared to the training and detection time. This may eventually lead to a neural network which is capable of near-real-time processing, which would greatly benefit the efficiency and productivity of rovers and similar systems.

Method

A labeled image dataset for deep learning-driven rock fall detection was selected for this study (Bickel 2021). The dataset contains the images with bounding boxes of the rockfalls since it was originally made to train detection systems. As this study is attempting to train a classification network, a new dataset was created by cropping and extracting smaller tiles either containing or not containing rockfalls. Tiles containing rockfalls (Figure 1) were cropped based on the provided bounding boxes, and empty tiles (Figure 2) were extracted from parts of the image not intersected by any boxes.

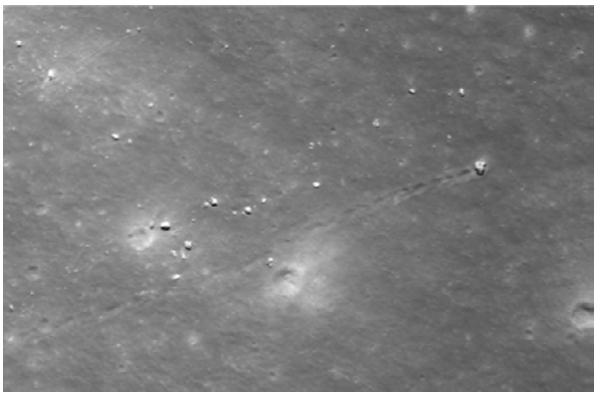

Figure 1: Image tile containing rockfall

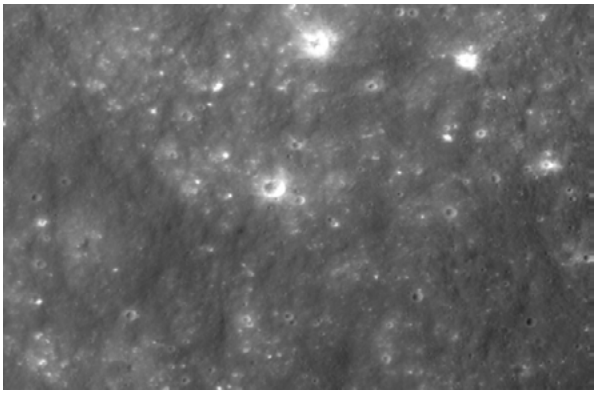

Figure 2: Image tile without any rockfalls

The new dataset was split into 80% training and 20% validation images. A large variety of off-the-shelf classification networks were chosen to be tested in this study. These include 2 unnamed CNNs, and Mobilenet, Resnet, and VGG16 transfer learning models. Each was trained for 100 epochs, with 30 steps, at a learning rate of 5e-5 using the Root Mean Squared Propagation (RMSprop) optimizer. The loss, accuracy, recall, precision, and F1 score, as well as training time per epoch and average classification time for 32 images of each model was recorded in order to make comparisons.

Results

The Resnet50 transfer learning model was found to perform the best, with a median recall, the highest precision, and the highest F1 score. The Mobilenet transfer learning model performed the fastest in both training time per epoch and detection time (Table 1 and Figure 3).

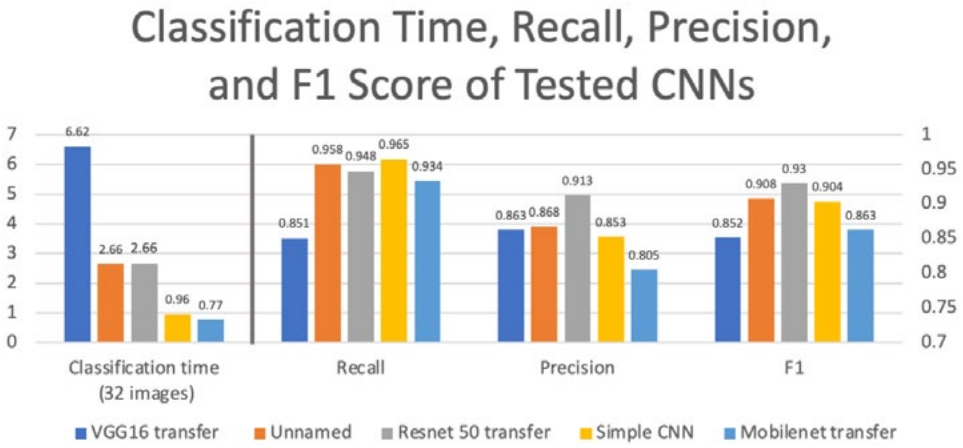

Figure 3: Chart of the classification time, recall, precision, and F1 score of the tested convolutional Neural Networks

Table 1: Performance of models in detecting rockfalls on Mars and the Moon

Model	Layers	Training time per epoch	Classification time (32 images)	Recall	Precision	F1
VGG16 transfer	18	7s	6.62s	0.851	0.863	0.852
Unnamed	50	38s	2.66s	0.958	0.868	0.908
Resnet 50 transfer	176	11s	2.66s	0.948	0.913	0.930
Simple CNN	16	11s	0.96s	0.965	0.853	0.904
Mobilenet transfer	85	6s	0.77s	0.934	0.805	0.863

Discussion

It appears that as classification time decreases, the recall approximately increases and the precision approximately decreases, indicating more correct predictions, but less rockfalls caught. This result matches expectations, since a more complex model should be able to classify more correctly. In comparison, a less complex model should be able to catch more, whether or not a rockfall is actually present. There also does not seem to be a direct relationship between the complexity, or amount of layers a model has, and the classification time. For example, VGG16 consists of 18 layers, and takes approximately 7 seconds to classify 32 images, while resnet50, with 176 layers, only takes approximately 3 seconds. This is likely due to the layer makeup of these networks, as different types of layers compute at differing speeds.

It was unexpected that the transfer learning models, or more specifically, VGG16 and Mobilenet, performed worse than the two unnamed models in both precision and F1. It was expected that the transfer learning models would perform worse in recall, as they should be less sensitive to noise, and thus would be expected to provide more false negatives in return for more correct positives. However, they also lack precision, meaning that they neither classify more, nor do they classify more correctly. There are a few possibilities as to why this could be. Firstly, these models were trained on color images, while the dataset used is in grayscale. Secondly, these models were trained for 1000-class classification, while in this study, they were just used for binary classification. Finally, it could be possible that the dataset these models were initially trained on, and the features they detected and kept, were unfit for detecting rockfalls.

Bickel et al. (2020) have performed a similar study with bounding box object detection networks on the same dataset. They were able to achieve a variety of tradeoffs between recall and precision, in the best case a recall of 0.6 to 0.07 and a precision of 0.39 to 0.95, and a maximum F1 score of 0.48. While comparisons can be made on various metrics, the two methods are fundamentally different, and should not be directly compared.

In conclusion, this study indicates that it is possible, though difficult, to achieve near-real-time processing of rockfalls in martian and lunar images. The HiRISE system collects images at approximately 213 megapixels per second (McEwen et al., 2007), while the fastest method tested could detect rockfalls at approximately 40 megapixels per second on the testing machine. As long as the system used to run these neural networks has approximately 5 times the processing power of the testing machine, super-real-time processing can be obtained. As well, processing speed can be increased by downscaling images. Depending on the requirements of a specific system, different networks or combinations of networks may be used. For example, a faster network with high recall and low precision may generate many potential areas to avoid for rover exploration, or generate safety and risk data for potential habitation candidates, as false positives would be better than false negatives. The fast speed would also be beneficial for full-planet analysis. A lower recall but higher precision network can be combined with a high recall network to improve speed, and would be able to be used in scientific research or targets for rovers, as false negatives would be more desirable than false positives.

Despite the significant contributions offered by the current study, there are some limitations which need to be addressed. The method employed in this study requires the large image to be cut into smaller sized blocks, which is required for these models to train on in a reasonable timeframe. Future studies with more computing resources may be able to train and test models on larger image patches. As well, further studies with more resources may be able to train the transfer learning models without transfer learning, thus computing features from scratch. These can then be compared against the current models, to investigate the effects of transfer learning on recall and precision. Finally, further studies may be able to train and test models that operate on bounding box networks, in order to compare the benefits and drawbacks of each method.

References

1. Bickel, V. T., Mandrake, L., & Doran, G. (2021). A Labeled Image Dataset for Deep Learning-Driven Rockfall Detection on the Moon and Mars, *Frontiers in Remote Sensing*, 2, https://doi.org/10.3389/frsen.2021.640034

2. Bickel, V. T., Conway, S. J., Tesson, P. -A., Manconi, A., Loew, S., & Mall, U. (2020). Deep Learning-Driven Detection and Mapping of Rockfalls on Mars. *IEEE Journal of Selected Topics in Applied Earth Observations and Remote Sensing*, 13, 2831-2841, https://doi.org/10.1109/JSTARS.2020.2991588.

3. Slade, S. (2021, March 22). *Stunning images of Mars keep coming 15 years after HiRISE camera first orbited the Red Planet*. The Washington Post. Retrieved January 31, 2022, from https://www.washingtonpost.com/lifestyle/kidspost/stunning-images-of-mars-keep-coming-15-years-since-hirise-camera-first-orbited-the-red-planet/2021/03/16/17af5e30-7c96-11eb-a976-c028a4215c78_story.html

4. McEwen, A. S., et al. (2007), Mars Reconnaissance Orbiter's High Resolution Imaging Science Experiment (HiRISE), J. Geophys. Res., 112, https://doi.org/10.1029/2005JE002605.

Chronic Traumatic Encephalopathy Among Athletes

By Elaine He

Author Bio

Elaine He is currently a high school junior at Sage Hill School, located in Orange County, California. She is interested in pursuing psychology or kinesiology/sports medicine as a college major, which is also reflected in AP Psychology being her favourite class. Outside of the classroom, Elaine is a versatile soccer player playing striker and center midfield for her high school team and defence for Slammers, a local club team. She competes with Sage Hill's MUN team and is a Co-President of SPIRIT, her school's volunteer organisation, and volunteers with the Tiger Woods Foundation in an effort to give back to others and to improve the quality of life for those less fortunate living in her community.

Abstract

Chronic Traumatic Encephalopathy (CTE) is a neurodegenerative disorder caused by the repetitive occurrence of mild Traumatic Brain Injuries (mTBI), commonly known as concussions, which remains a public health issue found most prevalent in high contact sports, specifically, American football. Typically, the severity of CTE is classified with McKee's staging scheme, which is mainly based on the degeneration and accumulation of p-tau neurofibrillary tangles in different parts of the brain. This refers to the unwound and clumped together tau proteins that are highly associated with CTE. The severity of the symptoms of stage I-IV can range from light headaches to a severe loss in motor and neural function. The underlying mechanisms and definitive biomarkers of CTE are still under debate, therefore, it cannot be diagnosed in vivo. Furthermore, external factors such as gender, age, and genetics (the presence of the ApoE4 allele) can affect both the severity and an individual's sensitivity to head trauma. However, interest in this topic has only recently begun to grow exponentially, and knowledge of CTE is still relatively preliminary. It has been shown to have overlapping biomarkers and symptoms with other neurodegenerative diseases such as Alzheimer's disease or Parkison's disease. Treatment of this issue so far has solely been preventative, as the development of medical therapies cannot proceed until CET can be diagnosed in vivo. The implication of education and stricter rules protecting athletes have been at the forefront of these measures.

Introduction

As head injuries become more normalised in high contact sports, a seemingly minor concussion every so often can quickly lead to more serious problems. Chronic Traumatic Encephalopathy (CTE) is a progressive tauopathy, or an abnormal amount of tau proteins in the brain that is associated with neurodegenerative disorders, caused by repetitive mild traumatic brain injuries, or concussions. It has been associated with aggression, depression, and the decline of many other cognitive functions among other symptoms. Additionally, CTE leads to a decrease in brain weight caused by a decline in the size of the cerebral cortex, temporal lobes, thalamus, brain stem, and other key regions of the brain (McKee et al., 2015).

Most commonly found in American football players and boxers- in addition to other high contact sports athletes e.g. soccer, wrestling, or rugby- concussions remain a prevalent problem in many professional leagues. Notably, the National Football League (NFL) raises concerns about concussions in many youth leagues. Additionally, CTE is also found in military personnel, with a significant number of combat injuries being head injuries (McKee et al., 2013).

Currently, the only way to definitively diagnose CTE is through autopsy, therefore, it is difficult to diagnose the disorder when an individual is still alive. Although there is no clear consensus on a specific diagnosis of CTE or the amount of trauma needed to cause it, the severity of symptoms correlated with it is defined by the density and regional distribution of p-tau, classified into four stages (I-IV) in McKee's staging scheme (McKee et al., 2015). Symptoms usually show 8-10 years after experiencing repeated head injuries and primarily progress with age, with older people tending to have higher CTE stages. The symptoms of stage I (mild) CTE are similar to those of concussions, including headaches or a loss of concentration and attention, but could also be asymptomatic. Similarly, stage II can also occasionally be asymptomatic, but additional symptoms included explosivity, short-term memory loss, and depression. In stage III, more cognitive impairments are found, such as apathy, memory loss, and executive dysfunction. Lastly, stage IV, the most severe stage, includes problems with motor functioning, aggression, word-finding difficulty, and has a strong association with dementia. CTE is often associated with other neurodegenerative disorders such as Alzheimer's, Motor Neuron Disease, or Parkinson's Disease. Similar to Alzheimer's Disease, where the ApoE4 allele has been associated with an increased risk of developing the disease, this allele is also speculated to affect the development of CTE (McKee et al., 2015).

Despite the recent growth in interest and research of CTE, much is still unknown about it. Given the importance of sports to human health and the prevalence of mild traumatic brain injuries in many of these popular activities, it is critical to identify the symptoms of a concussion and validate a set of criteria and underlying mechanisms for CTE, allowing the development and implementation of future preventative and recovery methods into different programs. In the following sections, an overview of the development and factors that affect both mTBI and CTE will be presented, followed by the prevalence of CTE in athletics. Based on empirical research, it is evident that CTE remains a major public health issue, primarily in high contact sports of all levels.

Development of Mild Traumatic Brain Injury (mTBI)

Given the millions of sports-related concussions estimated annually just in the United States, mild traumatic brain injuries, more commonly known as concussions, have been a major cause of concern for many athletes. It is one of the most common neurological disorders, accounting for around 90% of brain injuries (Saulle & Greenwald, 2012). Impact or a strong jolt to the head or shoulders, most common in sports like American football or boxing, if severe enough, can shift the brain to hit against the skull. This causes the stretching of axons along with a distortion in cellular membranes that cause the release of chemicals such as potassium and glutamate, and a depletion of intracellular energy stores which worsens the brain's metabolic dysfunction (McKee et al., 2013). mTBI is commonly defined as mild based on the Glasgow Coma Score, which categorises brain trauma as mild, moderate, and severe. Headaches, nausea, confusion, imbalance, and dizziness are some of the most common acute symptoms of concussions, which can be paired with a loss of consciousness, all

of which usually stop after a period of 1-6 weeks. However, during this period of metabolic dysfunction, an individual has a significantly higher vulnerability to a second concussion, which takes much longer to recover from as well as poses a long-term risk (Giza & Hovda 2001). Additionally, post-concussive syndrome (PCS) occasionally occurs, when symptoms of the concussion remain after three months since the injury, and usually lasts up to a year, though it could extend beyond this time frame in rare cases. In addition to the symptoms of concussions, many have also experienced emotional, cognitive, behavioural, and physical problems.

Concussion rates are generally highest in youth sports, besides the NFL, as the skulls and brains of minors are still developing during these years. Additionally, children with a history of concussion(s) generally have an increased risk of a slower recovery and longer symptoms after the injury, and this has been shown to have adverse effects on a student's academic performance, which emphasises the importance of adequate safety measures (Moser, 2002; Graham et al., 2001). Although these symptoms can be alleviated without medical intervention or long-term effects, the repeated or overlapping occurrence of the injury can lead to long-term consequences, namely, Chronic Traumatic Encephalopathy (Saulle & Greenwald, 2012).

Development of CTE

In contrast to the relatively straightforward timeline of mTBI, the development of CTE is not as direct, as in PCS does not directly lead to CTE. Given the axonal damage caused by repeated injuries, there are many shifts in the balance of the brain: membrane permeability, ionic shifts, and other chemical imbalances keep the brain in a prolonged state of hyperactivity that can lead to long-term neuron damage (McKee et al., 2013). Symptoms of CTE can be correlated with the specific part of the brain that is injured for example, damage to part of the hippocampal circuitry is associated with emotional, behavioural, or memory disturbances to the individual (McKee et al., 2012).

It is important to note that there is not yet a consensus on the exact mechanism of CTE. Typically, the emergence of CTE symptoms varies based on the individual and does not surface until later in life. In fact, some individuals were reported to be asymptomatic many years into retirement while others experienced symptoms only 4 years after they left their sport, while the youngest known individual with CTE was only 17 (McKee et al., 2013). The progression of symptoms follows a continuous decline in cognitive, emotional, and motor functions. Although at first, individuals affected may only experience concussion-like symptoms- poor concentration and attention, dizziness, headaches, disorientation, and memory problems, it can quickly progress to unstable behaviour in the form of outbursts and irritability, and speech issues. At this stage, a correlation between CTE and severe depression, suicide, and mood disorders, and the worsening of cognitive functions have been reported in previous research (Saulle & Greenwald, 2012). This proves to be devastating to the individuals affected as they often experience poor decision-making that can affect the people around them, such as divorce, relationship issues, abuse, drug addiction, paranoia, and bankruptcy to name a few. Finally, it can lead to a further loss in cognitive-motor functions where symptoms can resemble that of Parkinson's, Alzheimer's, dementia, and other neurodegenerative disorders (Mez et al., 2017).

The progression of CTE is captured by McKee's staging scheme, defined by stages I-IV, where stage I is the mildest stage and stage IV is the most severe (McKee et al., 2015). In accordance with the progression of CTE, corresponding pathological change can also be seen in the accumulation of p-tau neurofibrillary tangles(NFT) and the deterioration and change occurring within the brain. In stage I, abnormalities in p-tau are found in parts of the cerebral cortex but are minor, and the changes are still microscopic. These changes are associated with concussion-like symptoms. In stage II, there can be short-term memory loss and some emotional instability. There are more points of p-tau NFT in the cerebral sulci, and macroscopic changes begin to appear along with clusters of reactive microglia and axonal swelling. Stage III begins to show more macroscopic changes such as the reduction of brain weight and the enlargement of the third and lateral ventricles. The presence of NFT becomes more widespread, found in a majority of the key areas of the brain for example, the hippocampus, amygdala, frontal pole, and on occasion in the cerebellum and spinal cord grey matter. Finally, in stage IV,

the degeneration of the brain is readily apparent. Compared to the average 1,300-1,400 g brains, a brain weighing 1,000 g or less is not considered rare. There is atrophy, or a decrease of size, specifically in the frontal and temporal lobes, anterior thalamus, medial temporal lobes, white matter, and corpus callosum, to name a few. Additionally, p-tau is heavily distributed throughout the majority of the brain and a significant diminish in myelinated nerve fibres.

Currently, there is no definitive way to diagnose CTE, as it can only be diagnosed through autopsy. Due to its overlap in symptoms with other diseases, it is difficult to find specific biomarkers that can aid in making a diagnosis. However, there are speculations of different technologies and measurements to help define it, with advancements in neuroimaging, specifically diffusion tensor imaging (DTI) being one of the forefront technologies that many have hopes of using to detect changes associated with CTE (Saulle & Greenwald, 2012). DTI studies have shown to be sensitive enough to assess axonal structure and damage, and show changes in occult white matter that cannot be seen in other types of scans. Finally, several biomarkers have been proposed to diagnose CTE such as levels of change in glutamate, myoinositol, and tau levels among others.

p-tau and its Relevance to CTE

The presence of tau protein has been suggested to serve as a biomarker for neurodegenerative disorders, specifically Alzheimer's disease. However, because of the overlap between CTE and Alzheimer's, phosphorylated tau (p-tau) neurofibrillary tangles (NFT) inside brain cells have been used to track the progression of CTE. This occurs when the tau becomes hypophosphorylated and begins to unbind itself and disintegrate, clumping together to form these tangles. However, research has indicated that following traumatic brain injuries, the iron from bleeding is correlated to the formation of NTFs but are more associated with multiple mTBIs rather than one severe injury, overlapping the causes of CTE (Yoshiyama et. al, 2005).

CTE and mild TBI in the Context of Athletics

The majority of CTE cases have been reported in contact sports, notably, American football. One of the main figures in CTE research, Dr. McKee, is responsible for the development of the staging scheme (I-IV) of CTE and conducted one of the largest CTE studies in regards to football players, with 202 subjects (McKee, 2014, as cited in Mez et al., 2017). Out of these subjects, 87% (177 subjects) were diagnosed with CTE, and out of the 111 NFL players among the subjects, over 99% (110) were diagnosed. Out of these 110 subjects, 86% had severe CTE, with many of these individuals holding positions with significant helmet-to-helmet contact. In a smaller study of 34 NFL players, 89% of them had stage III or IV CTE with the mean development age of this disorder being 54. Another study showed a correspondence of CTE alongside neuropathological diseases such as Amyotrophic Lateral Sclerosis.

Furthermore, statistics about concussions in youth sports are still incomplete. Many of these studies do not include individuals below high school age and are more focused on football rather than other high school sports myoinositol. Out of the 700,000 (Gessel, 2017) concussions that occurred in United States high school athletics, 13.2 % were recurrent. It is important to note that many of these injuries go unreported. For a variety of reasons, a student may continue to play longer with a mTBI, greatly increasing their risk of recurrent concussions and long-term impairment that is often associated with CTE (Saulle & Greenwaldd 2012).

Internal and External Risk Factors among Different Populations in Concussions and CTE

Genetics have also been thought to be a factor in the development and severity of CTE, specifically, the presence of the ApoE4 allele (Saulle & Greenwald, 2012). In Alzheimer's Disease, the allele has been shown to increase the risk of developing the disorder. Given the overlap with CTE and Alzheimer's Disease, studies have shown that ApoE4 also has a role in the development of CTE, with many of the individuals with this allele having worse problems with head trauma (Saulle & Greenwald, 2012). Many studies have found a correlation with the allele and severe chronic impairment. Specifically, studies done by McKee & Omalu (2009) reported the presence of ApoE4 in the majority of the CTE cases studied (50%

and 70%) in each of their experiments. Furthermore, a study 2000 done by Kutner et al. found that older age and the presence of the genotype scored lower on cognitive tests than those without ApoE4.

Generally, females have a higher rate of concussions than males, even though males sustain more concussions as shown in a 2003 study. This study collected data from the NCAA Injury Surveillance System (ISS) over the period of three years, and concluded that out of 14,592 injured, 471 female athletes sustained concussion compared to 402 male athletes (Alosco et al., 2003). Additionally, on a high school level, the rates of concussions in girls' soccer (6.2%) were slightly higher than boys' soccer (5.7%). However, it is unclear as to why exactly this is the case. It is speculated that the higher rates can be attributed to females having weaker neck muscles than male athletes, or their smaller size, in the context of a greater ball-to-head size ratio (Covassin et al., 2003).

Finally, age, military involvement, lengths of years of playing, and the presence of the ApoE4 allele is speculated to affect the risk for the development of CTE. Soldiers are often exposed to head injuries in combat and exposed to certain toxins that can increase their risk of injuries (Saulle & Greenwald 2012). Given the higher risk nature of concussions in children due to their developing brains, it is a possibility that an injury can lead to a domino-like effect on destructive events through later years. However, this is not definitive, and conversely, the higher brain plasticity present in younger people could allow a better recovery than in adults. Years of athletic participation is also a risk factor for many athletes, with longer careers generally correlating to more severe CTE, presumably due to the positive correlation between the number of injuries and playing time (Lindsley 2017).

CTE vs Other Diseases

There is difficulty in defining CTE to create a clinical diagnosis due to the fact that its symptoms overlap with other diseases, which all may be traced back to head trauma such as Alzheimer's disease, Parkison's disease, and frontotemporal dementia (FTD) (Tartaglia et al., 2014). There is a strong overlap in the clinical and pathological features that define many of these diseases, and the presence of CET in an individual is often found alongside these other neurodegenerative diseases.

Treatment and Possible Future Research

Due to the somewhat preliminary stages of research on CTE, despite the significant growth of interest on this topic, treatment is still limited to preventative measures. However, in many sports such as American football and boxing, high contact is a part of what makes up the sport. Therefore, these measures need to be implemented within the practice of the sport. From stricter policies that penalise athletes from acting on overly aggressive or reckless plays to coaches educating both themselves and their players on the detrimental effects of mTBI, many suggest a change to these programs from an administrative level.

Another preventative measure entails an improvement of protective equipment. Studies have proven that newer helmets in American football were more protective and better at absorbing force than helmets in 1970, and the addition of more fitted, effective protective gear lowered the impact of an individual's body; Additionally, there has recently been an interest in neck strength and its correlation to injury strength[CITATION]. Cognitive rehabilitation therapy (CRT) and other medical therapies are continuing to be developed to limit damage after injury and aid in recovery. However, much of these developments will heavily benefit from a definitive pathological definition and diagnostic criteria of CTE, which is something only future research can help clarify.

Summary

Chronic Traumatic Encephalopathy (CTE), a progressive tauopathy caused by repetitive mTBIs, or concussions, has been associated with aggression, depression, and the decline of many other cognitive functions among many other symptoms. Its prevalence in high contact sports that many view as an essential part of childhood and culture, specifically American football, is a cause of concern to many of these athletes. CTE is defined into 4 stages by a framework developed by Dr. McKee, Dr. McKee's studies show that 99% of NFL participants have CTE, with the majority of them having stage III-IV CTE. These stages are often associated with other neurodegenerative diseases such as Alzheimer's, Parkison's, Motor Neuron Disease, and FDT.

However, due to the absence of definitive biomarkers and the underlying mechanisms of CTE, it currently can only be confirmed with an autopsy and not be diagnosed when a patient is alive. Despite the relatively preliminary knowledge of CTE, existing research has revealed risk factors such as age, gender, occupation, and the presence of the ApoE genotype, which increased the severity of the symptoms of concussions and hindered cognitive function in many football players. The identification and validation of a criteria and underlying mechanisms for CTE is essential to the development and implication of future preventative and recovery methods into different programs.

References

1. Alosco, M. L., Cherry, J. D., Huber, B. R., Tripodis, Y., Baucom, Z., Kowall, N. W., ... & Covassin, T., Swanik, C. B., & Sachs, M. L. (2003). Sex differences and the incidence of concussions among collegiate athletes. *Journal of athletic training*, 38(3), 238.

2. Graham, R., Rivara, F. P., Ford, M. A., Spicer, C., & Graham, R. (2014). Sports-related concussions in youth. *National Research Council and Institute of Medicine*

3. *Sports-Related Concussions in Youth: Improving the Science, Changing the Culture*, 309-330.

4. Giza, C. C., & Hovda, D. A. (2001, September). *The neurometabolic cascade of concussion*. Journal of athletic training. Retrieved January 4, 2022, from https://www.ncbi.nlm.nih.gov/pmc/articles/PMC155411/

5. Lindsley, C. W. (2017). Chronic traumatic encephalopathy (CTE): a brief historical overview and recent focus on NFL players.

6. McKee, A. C., Stein, T. D., Kiernan, P. T., & Alvarez, V. E. (2015). The neuropathology of chronic traumatic encephalopathy. *Brain pathology*, 25(3), 350-364

7. McKee, A. C., Stein, T. D., Nowinski, C. J., Stern, R. A., Daneshvar, D. H., Alvarez, V. E., ... & Cantu, R. C. (2013). The spectrum of disease in chronic traumatic encephalopathy. *Brain*, 136(1), 43-64.

8. McKee, A. C. (2020). Characterizing tau deposition in chronic traumatic encephalopathy (CTE): utility of the McKee CTE staging scheme. *Acta Neuropathologica*, 140(4), 495-512.

9. Mez, J., Daneshvar, D. H., Kiernan, P. T., Abdolmohammadi, B., Alvarez, V. E., Huber, B. R., …& McKee, A. C. (2017). Clinicopathological evaluation of chronic traumatic encephalopathy in players of American football. *Jama*, 318(4), 360-370.

10. Moser, R. S., & Schatz, P. (2002). Enduring effects of concussion in youth athletes. *Archives of Clinical Neuropsychology*, 17(1), 91-100.

11. Saulle, M., & Greenwald, B. D. (2012). Chronic Traumatic Encephalopathy: A Review. *Rehabilitation Research and Practice*, 2012, 1–9. https://doi.org/10.1155/2012/816069

12. Tartaglia, M. C., Hazrati, L. N., Davis, K. D., Green, R. E., Wennberg, R., Mikulis, D., ... & Tator, C. (2014). Chronic traumatic encephalopathy and other neurodegenerative proteinopathies. *Frontiers in human neuroscience*, 8, 30.

13. Yoshiyama, Y., Uryu, K., Higuchi, M., Longhi, L., Hoover, R., Fujimoto, S., McIntosh, T., Lee, V. M. Y., & Trojanowski, J. Q. (2005). Enhanced Neurofibrillary Tangle Formation, Cerebral Atrophy, and Cognitive Deficits Induced by Repetitive Mild Brain Injury in a Transgenic Tauopathy Mouse Model. *Journal of Neurotrauma*, 22(10), 1134–1141. https://doi.org/10.1089/neu.2005.22.1134

Chi-Squared Analysis of the Uncertainty of Falling Chain Experiments

By David Hu

Author Bio

David Hu is a native of Tallahassee, Florida, and grew up in western Pennsylvania. He is currently attending Slippery Rock Area High School in PA. His favorite subject is physics, and he is particularly interested in aerospace engineering. In his school, David is part of the varsity soccer team as well as the track & field team where he does pole vault. He leads the school's National Honors Society (NHS). He is a treasurer of multiple school clubs and a member of German National Honor Society. In his spare time, he enjoys listening to music, making films, and hiking in nature.

Abstract

The falling chain problem is a classic physics problem that studies the dynamics of a chain falling in a gravitational field. There are different ways to investigate the problem. One of them is a U-Chain system in which a chain is attached to a rigid support by its two ends. As one of the ends is released, the chain begins to fall. Various models have been suggested to explain the acceleration of the falling end in a U-Chain system, but few of these analyses have determined a best-fit model and fewer still have tested their models. In this project, a one-parameter chi-squared analysis is used to test a model that describes the relationship between the falling time of one end of U-chains and their lengths. The falling of five chains is recorded and used in the experiment. A best-fit model was obtained, but was not a good fit to the data, despite only a small difference between the best-fit and model-predicted parameter values. The lack of a good fit is attributed to underestimated measurement uncertainties due to the measurement method. The fact that a good fit was not obtained despite only a small difference between best-fit and model-predicted parameter values is evidence of the sensitivity of chi-squared model testing.

Keywords: Falling Chain, Chi-Squared Analysis, Uncertainty, Best-Fit Model, Kinetic Energy, Potential Energy, Goodness of Fit, Standard Error

Introduction

The falling chain problem was studied as early as the 19th century (Cayley, 1857). There are two well-known falling chain problems, U-chain and pile-chain (de Sousa et al., 2012). In the U-chain system, a flexible heavy chain is attached to a rigid support by its two ends. As one of the ends is released, the chain begins to fall. It is found that if the distance between the two ends is small compared with the length of the chain, the falling end will accelerate faster than gravitational acceleration g. In the pile-chain system, a chain is compacted together in a heap and one end is brought over the edge of a table and starts falling with an acceleration of g/3 (de Sousa et al., 2012; Tomaszewski et al., 2006).

The falling chain problem can be studied using chains with different lengths, different weights, or both. Wong and Yasui (2006) indicated that energy conservation arises because the links are transferred by elastic collisions as opposed to inelastic collisions. They found that the end of a falling chain accelerates faster than g due to the part of the chain right under the falling end which pulls the falling end down further. Géminard and Vanel (2008) analyzed the tip of a freely falling chain in a gravitational field where one end is suspended and concluded that the time-resolved measurements of horizontal and vertical components complement previous laboratory and simulations of free-end dynamics. Clouser and Oberla's experiment (2008) showed that energy is not conserved due to inelastic collisions. De Sousa et al. (2012) analyzed the theoretical and experimental data of a falling U-chain and a pile-chain. They found that a two sub-system model based on energy conservation provided a good fit to the data. Pantaleone (2019) developed a simple model to measure the size of the tension that pulls the chain downwards based on the length and width of a link, the maximum beading angle at a junction, and the inclination angle of the surface and the coefficients of friction and restitution between the chain and the surface.

While most of the previous studies have centered on the explanation of the acceleration of different falling chains using different theories in physics, few studies have considered if the model represents the data well and if the data collected is good enough to represent the phenomenon that we are studying. These questions are about the randomness and uncertainty in the process of data collecting and modeling in physics experiments. Different methods have been used to evaluate modeling results. Chi-squared (X2) analysis is one of them.

Chi-squared analysis is a statistical analysis used to compare actual results with an expected hypothesis. It combines both curve-fitting and model-testing by considering measurement uncertainties. Hence, chi-squared analysis can estimate model parameter values and test a model's goodness-of-fit. The two most used versions of this analysis method are the chi-square goodness of fit test and the chi-square test of independence. Witkov and Zengel (2019) used chi-squared analysis to test a one-parameter linear model (y=Ax) that estimated the ratio of the maximum force when a chain is falling onto a scale to the weight of the chain. In their study, y is the maximum force. x is the weight of the chain. A is 3. That is, in a theoretical condition, when a chain falls on a scale, the maximum force is 3 times the weight of the whole chain. One-parameter chi-squared analysis was applied on the data collected by the authors. A best fit model of y=2.96x was obtained, very close to the theoretical model. The result of the chi-squared analysis also indicated that the model was a good fit because it fell within two standard errors of the best fit parameter. The case study proved that chi-squared analysis is a very useful tool to evaluate models and uncertainties in data collection. Currently, no study has used chi-squared analysis to test models regarding the fall time in falling chain problems.

Therefore, in this project, the chi-square goodness of fit analysis was applied to evaluate a model of a U-chain system. The objectives of this study are to obtain a best-fit parameter value (i.e., slope) for a theoretical model and to examine if the best-fit is a good fit to the collected data.

Research Methodology

A Theoretical Model of U-Chain Falling System

In this project, a U-chain system is used. That is, a chain is attached to a rigid support by its two ends. As one of the ends is released, the chain begins to fall (Figure 1). According to C. Witkov (personal

communication, July 24, 2021), a theoretical model has been derived that represents the relationship between the length of the chain (L) and the time the falling end reaches the lowest point (T). This theoretical model is based on the potential and kinetic energy of both sides of the chain. The main steps of the model derivation are as below:

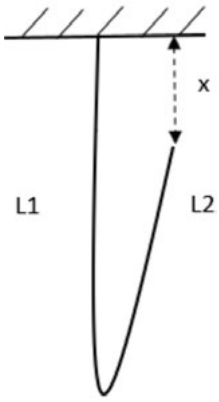

Figure 1. Schematic of a falling chain

L_1: *the length of the left portion of the chain*
L_2: *the length of the right portion of the chain*
x: *the distance between the rigid support and the falling end*

Step 1: When both ends are attached to the rigid support, the left and right portion have the same length.

$$L_1 = L_2 = \frac{L}{2} \quad (1)$$

Step 2: When the right end of the chain starts falling, the length of the left side will be increasing, and the right side will be decreasing.

$$L_1 = \frac{L}{2} + \frac{x}{2} = \frac{L+x}{2} \quad (2)$$

$$L_2 = \frac{L}{2} - \frac{x}{2} = \frac{L-x}{2} \quad (3)$$

Step 3: When the right end is falling, the potential energy of both sides will also be changing.

$$U_1 = -m_1 g h_1 \quad (4)$$

$$U_2 = -m_2 g h_2 \quad (5)$$

where, U_1 and U_2 are the potential energy of the left and right portion of the chain respectively, m_1 and m_2 are the mass of the left and right portion of the chain respectively, g is the gravity of the Earth, and h_1 and h_2 are the center of the mass of the left and right respectively. m_1, m_2, h_1,and h_2 can be decided using the following equations:

$$m_1 = \mu L_1 = \frac{\mu(L+x)}{2} \quad (6)$$

$$m_2 = \mu L_2 = \frac{\mu(L-x)}{2} \quad (7)$$

where, μ is the linear density.

$$h_1 = \frac{1}{2}L_1 = \frac{\left(\frac{1}{2}\right)(L+x)}{2} \quad (8)$$

$$h_2 = x + \frac{1}{2}L_2 = x + \frac{\left(\frac{1}{2}\right)(L-x)}{2} \quad (9)$$

Then,

$$U_1 = -\left(\frac{\mu g}{8}\right)\left(L^2 + 2Lx + x^2\right) \quad (10)$$

$$U_2 = -\left(\frac{\mu g}{8}\right)(2Lx + L^2 - 3x^2) \quad (11)$$

So, the total potential energy of both sides, Utotal, is as below:

$$U_{total} = U_1 + U_2 = -\left(\frac{\mu g}{4}\right)(L^2 + 2Lx - x^2) \quad (12)$$

Step 4: As the right side of the chain is moving, there is also the kinetic energy on the right side calculated as below:

$$K_2 = \frac{1}{2}m_2 v^2 = \frac{\mu(L-x)}{4}v^2 \quad (13)$$

where K2 is the kinetic energy of the right portion of the chain, and v is the velocity of the falling end of the chain, and $v = \frac{dx}{dt}$

Step 5: Based on the law of energy conservation, the initial energy (Ei) equals the final energy (E_f). And the total energy (E) at any given time is the sum of kinetic energy (K) and potential energy (U). Therefore,

$$K_i + U_i = K_f + U_f \quad (14)$$

where, K_i and K_f are the initial and final kinetic energy respectively, and U_i and U_f are the initial and final potential energy respectively.

As the initial kinetic energy is 0 when x=0, the above equation can be written in the following format:

$$0 + \left(-\frac{\mu g}{4}\right)\left(L^2\right) = \left(\frac{\mu}{4}\right)(L - x)v^2 + \left(-\frac{\mu g}{4}\right)(L^2 + 2Lx - x^2) \quad (15)$$

Then,

$$(L - x)v^2 = 2gLx - gx^2 \quad (16)$$

$$v = \frac{dx}{dt} = \sqrt{gL}\sqrt{\frac{2\left(\frac{x}{L}\right)-\left(\frac{x}{L}\right)^2}{1-\frac{x}{L}}} \quad (17)$$

$$\frac{dx}{\sqrt{\frac{2\left(\frac{x}{L}\right)-\left(\frac{x}{L}\right)^2}{1-\frac{x}{L}}}} = \sqrt{gL}\,dt \quad (18)$$

Step 6: Derive the theoretical model by integrating both sides of the above equation.

$$\int_0^1 \sqrt{\frac{1-\frac{x}{L}}{\left[2\left(\frac{x}{L}\right)-\left(\frac{x}{L}\right)^2\right]}}\, d\left(\frac{x}{L}\right) = \int_0^{t_F} \sqrt{\frac{g}{L}}\, dt \quad (19)$$

where, t_F is the final time. Then,

$$1.19814 = \sqrt{\frac{g}{L}}\, t_F \quad (20)$$

Since g=9.8 m/s2 , the theoretical model is:

$$t_F = 0.38\sqrt{L} \quad (21)$$

Videos of falling chain experiments

Five videos of a falling chain process were recorded. Each video used a different chain length. The original video is 400 frames per second (fps). To be able to measure the time of the falling chains, the videos were converted to a slow motion of 30 fps.

Timing strategy

Time was measured between the start and end of the falling process using the stopwatch function on a commercially available cell phone. Five repeated and independent measurements were performed for each of the five falling chain videos. Since the frame rate of the video is not real-time, actual time was calculated using Equation 22.

$$Actual\ time = \left(\frac{30fps}{400fps}\right) video\ time\ from\ stopwatch \quad (22)$$

Apply the above data in chi-squared goodness of fit analysis

Chi-squared goodness of fit analysis is based on a Gaussian distribution of uncertainties around each data point and the central limit theorem (Witkov & Zengel, 2019). The equation of chi-squared analysis is defined as

$$X^2 = \frac{\sum\left(y_i - y_{model_i}\right)^2}{\sigma_i^2} \quad (23)$$

where, σ_i is the standard error of the mean in the measurement, representing the uncertainty of the ith measurement. depends on the number of measurements (N) and the root-mean-square deviation (RMSD) of the data.

$$\sigma_i = \frac{RMSD}{\sqrt{N}} \quad (24)$$

In the case of a one-parameter linear model, the X^2 is defined as

$$X^2 = \frac{\sum_i \left(y_i - Ax_i\right)^2}{\sigma_i^2} \quad (25)$$

The best fit value of the slope A is the one that minimizes X^2. But, the best fit model is not necessarily a good fit to the data. Chi-squared analysis assumes that uncertainties on x are negligible and only the uncertainties on y are evaluated. Considering the uncertainty in measurements, a model is a good fit to the data if most of the measurements are within one of the line of best fit. The minimum value of X^2 (X^2_{min}) can then be determined based on one σ from the best-fit model. If

$$y_i = y_{model_i} \pm 1\sigma_i = Ax_i \pm 1\sigma_i \quad (26)$$

Then,

$$X^2 = \frac{\sum_i^N (y_i - Ax_i)^2}{\sigma_i^2} = \frac{\sum_i^N (Ax_i \pm 1\sigma_i - Ax_i)^2}{\sigma_i^2} = \sum_i^N 1 = N \quad (27)$$

According to Equation 27, if a model is a good fit to the data, the X^2_{min} should be around the order of N.

$$X^2_{min} \approx N \text{ for a good fit} \quad (28)$$

Therefore, any value that is within N±2N is a good value of X^2_{min}.

Chi-squared analysis also provides an uncertainty estimate for the best fit parameter. A model will be rejected if the parameter A in the theoretical model is more than two standard deviations (Aσ) of the Gaussian distribution of the best fit parameter value (A_{best}). That is, the uncertainty of Abest is represented as A_{best}±2Aσ. This uncertainty can be found by examining the interception between X^2_{min}+4 and a X^2(A) parabola.

To test the model and data collected in this project, the chains' lengths and their falling times from the above steps were brought into the script of one-parameter chi-squared analysis developed by Witkov and Zengel (2017).

Results

The five chains' lengths, the falling times from the stopwatch, and the actual times each chain took to fall to the bottom are shown in Table 1.

	Chain 1		Chain 2		Chain 3		Chain 4		Chain 5	
Length	0.781m		1.076m		1.314m		1.596m		1.841m	
Time (s)	**Video Time**	**Actual Time**	**Video Time**	**Actual Time**	**Video Time**	**Actual Time**	**Video Time**	**Actual Time**	**Video Time**	**Actual Time**
Time 1	4.35	0.326	4.66	0.350	5.46	0.410	6.16	0.462	7.05	0.529
Time 2	4.39	0.329	4.71	0.353	5.53	0.415	6.08	0.456	6.87	0.515
Time 3	4.34	0.326	4.75	0.356	5.57	0.418	6.10	0.458	7.01	0.526
Time 4	4.22	0.317	4.74	0.356	5.60	0.420	6.15	0.461	6.86	0.515
Time 5	4.40	0.330	4.77	0.358	5.49	0.412	6.04	0.453	6.98	0.524

The chains' lengths are filled in the script as the x-variable arrays (independent variable) and the five measurements of each chain's falling time are used as the y-variable arrays (dependent variable) (Table 2).

Table 2 Filling variable arrays in the script

Variable arrays	Values
Independent variable (x)	[0.781, 1.076, 1.314, 1,596, 1.841]
Dependent variable 1 (y)	[0.326, 0.329, 0.326, 0.317, 0.330]
Dependent variable 2 (y)	[0.350, 0.353, 0.356, 0.356, 0.358]
Dependent variable 3 (y)	[0.410, 0.415, 0.418, 0.420, 0.412]
Dependent variable 4 (y)	[0.462, 0.456, 0.458, 0.461, 0.453]
Dependent variable 5 (y)	[0.529, 0.515, 0.526, 0.515, 0.524]

The results from chi-squared analysis (Figure 2) indicate that the best fit parameter A_{best} is 0.36 and the minimum value of X^2 is 329.59.

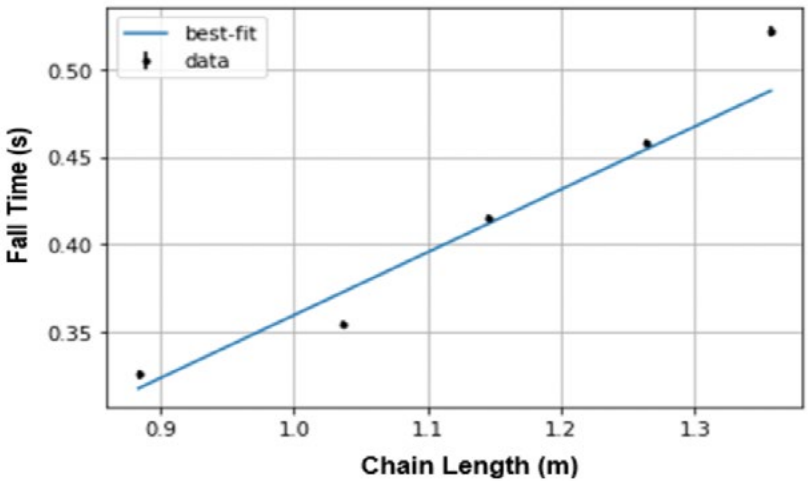

Figure 2
Falling chain data plot

Running the script of chi-squared analysis also created a X2 plot (Figure 3):

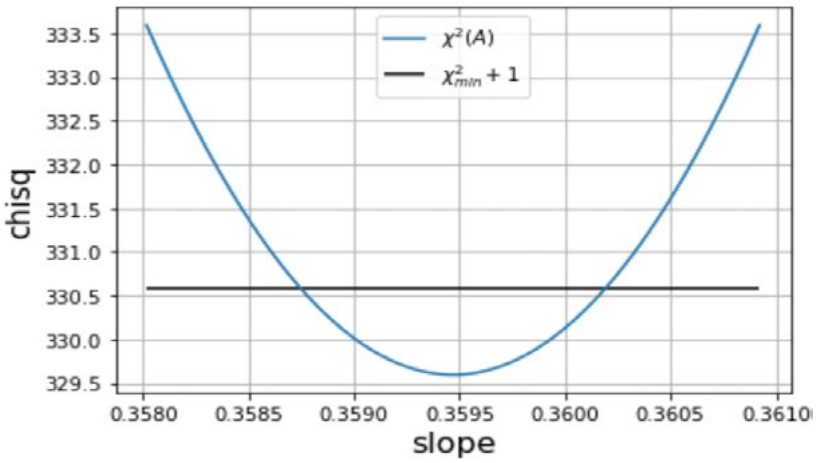

Figure 3
Falling chain X^2 plot

Discussion and Conclusion

This study represents the first research applying chi-squared analysis to the classic problem of falling U-chain. Running the chi-squared analysis script gives the best-fit parameter A_{best}=0.36, indicating that the model y=0.36x is a best-fit to the data. However, the X^2_{min} is 329.59, far beyond the required range of a good fit, which is between 1.84 and 8.16 $(N\pm\sqrt{2N})$. This means that this model is not a good fit to the data collected.

A major reason of the high value of X^2_{min} is that measurement uncertainties are underestimated in this experiment due to the measurement method such as human recording of a stopwatch and measuring time from videos instead of actual chain falling. From the definition of chi-squared analysis, underestimation of uncertainties leads to overestimation of chi-squared values (including the minimum value of chi-squared).

As a result of chi-squared analysis including measurement uncertainties in its definition, one of the attractive features of chi-squared analysis is that failure to meet its good-fit criteria reveals information not only about the model, but also about the experiment used to test the model.

The close numerical match between the best-fit parameter value (A_{best}=0.36) and the theoretical parameter value (A=0.38) despite failing the goodness-of-fit test demonstrates the sensitivity of chi-squared model testing to both the model and correctly estimating measurement uncertainties.

Based on the inspection of the interception between X^2_{min}+4 and the $X^2(A)$ parabola in Figure 3, the uncertainty of A_{best} , represented as $A_{best}\pm2\sigma_A$, is determined to be between 0.3580 and 0.3609, which does not contain the parameter A of the theoretical model, 0.38. This further confirms that the model is rejected.

This project demonstrates that chi-squared analysis is a very useful tool for model testing and uncertainty measurement. In this work, chi-squared analysis is applied to the falling chain problem. The results indicate that the model is a best-fit, but not a good fit to the data, and that high uncertainties exist in the measurement of A_{best} . To improve the model fit in a future study, the measurement method may be modified, such as testing the falling time directly from a falling chain instead of using videos, using high-resolution videos, using some auto-tracking programs to measure falling time, and increasing the number of chains used in the experiment. Furthermore, air resistance may be considered in the derivation of the theoretical model.

Acknowledgement

I would like to express my sincere gratitude and appreciation to Dr. Carey Witkov for patiently guiding me through this research project. I would also like to thank Dr. Zhaonan Sun for his assistance in my paper writing process.

Bibliography

1. Cayley, A. (1857). VIII. On a class of dynamical problems. *Proceedings of the Royal Society of London*, 8, 506–511. https://doi.org/10.1098/rspl.1856.0133

2. Clouser, B., & Oberla, E. (2008). *The Falling Chain Problem*. http://hep.uchicago.edu/~eric/work/docs/requiemForARosner.pdf

3. de Sousa, C. A., Gordo, P. M., & Costa, P. (2012). Falling chains as variable mass systems: Theoretical model and experimental analysis. *European Journal of Physics*, 33(4), 1007–1020. https://doi.org/10.1088/0143-0807/33/4/1007

4. Géminard, J.-C., & Vanel, L. (2008). The motion of a freely falling chain tip: force measurements. American Journal of Physics, 76(6), 541–545. https://doi.org/10.1119/1.2870271

5. Pantaleone, J. (2019). Understanding how a falling ball chain can be speeded up by impact onto a surface. Proceedings of the Royal Society A: Mathematical, Physical and Engineering Sciences, 475(2223), 20180578. https://doi.org/10.1098/rspa.2018.0578

6. Tomaszewski, W., Pieranski, P., & Geminard, J.-C. (2006). The motion of a freely falling chain tip. *American Journal of Physics*, 74(9), 776–783. https://doi.org/10.1119/1.2204074

7. Witkov, C., & Zengel, K. (2017). *Script of chi-squared curve fitting to a 1-parameter linear model* [Github]. https://github.com/witkov/scripts/blob/master/falling_chain.ipynb

8. Witkov, C., & Zengel, K. (2019). *Chi-Squared Data Analysis and Model Testing for Beginners*. Oxford University Press; Illustrated edition.

9. Wong, C. W., & Yasui, K. (2006). Falling chains. *American Journal of Physics*, 74(6), 490–496. https://doi.org/10.1119/1.2186686

Accessing the impact of negative externalities from Concentrated Animal Feeding Operations in China

By Shu Jun Liu

Abstract

Concentrated animal feeding operations (CAFOs) have emerged as a result of the rapid industrialization of the livestock sector five decades ago, leading to positives such as increased global food security and negatives: massive point source pollution sites, potential human health effects, and questions over animal cruelty. Though much research has been published in the United States regarding these harms, this paper specifically focuses on trends and pollution from the livestock industry in China. With data gathered from the National Bureau of Statistics, the statistical database for China, and the World Bank, I analyze four geographical areas with differing outputs of meat, which I use as a proxy for the number of CAFOs in a region. The findings reveal a strong and positive correlation between the output of meat and pollutants. My results show that it is certainly plausible for livestock to be a strong contributor to the varying levels of observed pollutants.

Keywords: CAFOs, Livestock, Pollutants, Greenhouse gases, Manure, Environment, Green technology, Meat production

Introduction

In recent decades, China has emerged as the world's leading producer of livestock, overtaking the United States and Europe. Growing demand, driven by a growing population, technological innovation, and improved infrastructure has fueled the expansion of the livestock sector, resulting in impressive aggregates of total industry output (Bai et al., 2018). The gross output value of animal husbandry in China has increased by 13612.4% from 1978 to 2018 (3.23 billion USD to 442.91 billion USD).

As with many industries, the livestock sector has industrialized, from small-scale family farms into large industrial complexes. Concentrated animal feeding operations (CAFOs) are an intensive version of animal feeding operations (AFOs), where at least 1000 animal units, equivalent to one million pounds of animal weight, are confined for over 45 days per year in an area without vegetation (United States Environmental Protection Agency, 2021). Recently, the scrutiny has been placed on these operations as a result of agriculture being identified as a driving factor of climate change.

This paper focuses on negative externalities produced by CAFOs in China. Negative externalities are the costs on third-party members not included in the production costs of the agent who generates the externalities. The specific lens on pollution within negative externalities has been chosen due to the extensive harmful effects that pollution from these operations imposes on surrounding communities. The plethora of impacts created by CAFOs have been studied at length in various contexts, but the vast majority of studies focus on operations in the Midwest of the United States. Within China, research concentrates on aquatic pollution and the potential health impacts of antibiotics which are biomagnified up the food chain to affect human and animal life. Although growing emphasis has been placed on mitigation of harmful environmental impacts, to my knowledge, no comprehensive study on externalities from water and atmospheric pollution specifically in the context of China has been published.

CAFOs are the epitome of industrialization's response to traditional agriculture. When properly managed, the phenomenon generates economies of scale and efficiency. In the United States, it has allowed for milk production to double, meat production to triple, and egg production to increase fourfold since the 1960s (Delgado et al., 2003). The operation's goal is to maximize output while minimizing costs, effectively resulting in low-cost animal products and production, easier management of animals, and less resource consumption in relation to family-operated livestock farms. Animals are fed specialized feed and antibiotics to speed growth – in comparison to the 1920s, chickens can reach more than double the size in less than half the time (Pew, 2009).

Yet, this process has also led to massive tradeoffs with the environment and transformative global impacts. Total greenhouse gas emissions in China increased more than two-fold, from 233 to 520 tera-grams of carbon dioxide equivalent between 1980 and 2010 in the livestock sector (Bai et al., 2018). The amount of feces and urine resulting from the smallest CAFO is equivalent to that of 16,000 humans, which leads to continual questions regarding waste disposal and treatment. This waste is not always treated properly to rid it of possible pathogens and antibiotics present in the matter, which can lead to severe and adverse impacts on human and animal health (Hribar, 2010). Moreover, the number of nutrients contained in fecal matter, such as nitrogen and phosphorous, can lead to harmful algal blooms in nearby streams and bodies of water.

The environmental harms which result from the advent of the operations described here have been increasingly highlighted as the world becomes more aware of sustainability issues. The aim of this paper is to identify the numerous negative externalities associated with producing livestock at CAFOs. A summary of the findings is this: there are strong positive correlations between livestock production and four major pollutants in wastewater and waste gas in China. From this, it is certainly plausible to assume that livestock production, which arises from CAFOs, contributes to the concentration of pollutants in four distinctive areas: Shanghai, Jiangxi, Hunan, Shandong.

The paper is organized as follows: in section 2, I explore previous work on CAFOs and the externalities they generate; further, I highlight how my findings fill a gap in the literature. In section 3, I introduce the data and its sources; in section 4 I present the empirical findings; section 5 is the conclusion.

Literature Review

Livestock Trends

Worldwide, the agricultural and livestock sectors have undergone significant transformations. Although it is one of the last means of production to industrialize, the livestock sector has experienced massive and standardized changes in the raising of animals. The trends indicate that despite an overall reduction in the number of total farms, there has been an overall increase in the concentration of animals and size of each farm (Copeland, 2010; Donham et al., 2007; Ikerd, 2013). This pattern points toward an industry-wide switch to large-scale factory farms. In the United States, between the years 1980 to 2008, the number of beef cattle, hog farms, and dairy farms fell by 41, 90, and 80 percent, respectively (The United States Department of Justice, 2020). However, between 1982 and 1997, the number of animals at singular feeding operations rose by 88 percent, coupled with an increase of more than 50 percent for the number of CAFOs (U.S. Department of Agriculture, 2000). Although this statistic is for the United States, it is applicable for China as both countries have undergone very similar trends in livestock production, and have nearly identical values on the livestock production index (World Bank, 2018).

Manure Management

Manure is typically beneficial for agriculture, serving as fertilizer to stimulate growth for new crops. However, the sheer amount of animal waste produced at CAFOs creates many problems, including disposal of increasingly large quantities of manure, and management of the many contaminants found in it. Typically, manure is first stored in lagoons, and then it is applied to land (Nicole, 2013). The storage process has many pitfalls — e.g., the lagoons all leach to some degree — and during storms, waste can burst or spill into surrounding fields or waterways (Nicole, 2013). As no sewage treatment process exists, there are over 150 pathogens in animal manure that may impact human health. Once the manure is applied to soil, these pathogens can survive for up to two months, creating the possibility of contaminating our food source and water (Hribar, 2010; Hu et al., 2017).

The application of manure to land creates a multitude of problems. The land cannot properly absorb the nutrients as fertilizer since the waste is typically overapplied. While there is an established threshold of 30 tons/hm^2 of animal waste loading on land to preserve land quality in China, six provinces have already overshot this guideline (Hu et al. 2017). Furthermore, the excess nutrients easily runoff into nearby bodies of water, causing pollution which severely damages aquatic life (Burkholder et al., 2007; Hu et al., 2017; Ikerd., 2013; Wing et al., 2013).

Water pollution

River contamination has been recorded during severe weather conditions, including manure spillage from lagoons or other containment methods. The impacts of such accidents are long-lasting and severe: over 35,000 miles of river have been polluted in the US, resulting in massive dead zones[1] from algal blooms, fish kills, and bacterial contamination (Burkholder et al., 2007; Gurian-Sherman, 2008; Ikerd, 2013). In 2005, a storage lagoon in upstate New York spilled, with millions of gallons of manure ending up in the Black River, resulting in an estimated 375,000 fish deaths (New York State Department of Environmental Conservation, 2007). In Jiyun River, a river in Beijing, which flows through the central meat-producing counties, research sampling has found that there are 2 to 4 times above-normal antibiotic levels in the water, which can negatively impact both aquatic and human health (Zhang et al., 2014).

Other than these specific point-source incidents, excess nutrients from the land application of manure also frequently end up in surface and underground water sources. For surface water contamination, wind and rain often move manure components into waterways; direct discharging of manure into water is also practiced. Overloading the water with nutrients and increasing water turbidity[2] can seriously impact aquatic life by changing these organisms' established environments (Copeland, 2010). Manure also has the potential to percolate

[1]Areas where the amount of dissolved oxygen in water is unable to support most marine life.

[2]A measure of the amount of suspended matter or relative clarity of water

into soils and affect groundwater quality. In China, 62 percent of wells were found to exceed the nitrate standard set by the World Health Organization (WHO), with the main identified sources of nitrate coming from manure and fertilizer (Bai et al., 2017).

Air pollution

In addition to water pollution, CAFOs also emit greenhouse gases that disrupt the atmosphere. Animal activities, from breathing to handling to feeding, and animal waste, are all sources of Volatile Organic Compounds (VOCs)[3] that can negatively impact both the environment and human health (Yuan et al., 2017). Air quality assessments around factory farms reveal concentrations of ammonia and hydrogen sulfide that are above the limits set by the US Environmental Protection Agency and can affect surrounding areas within 1km of poultry farms (Donham et al., 2006; Hu et al., 2017). Animal manure accounts for 75 percent of ammonia emissions from agriculture in the European Union (Bittman et al., 2014). As it assimilates into the atmosphere, ammonia has the potential to react with other atmospheric pollutants such as sulfur dioxide and nitrogen oxides and can spread to regions as far as 1000km (Asman et al., 1998, Fowler et al., 1998).

Health effects

Studies have shown that workers at CAFOs are subject to adverse health effects – 25 percent reported developing respiratory illnesses such as asthma and organic dust toxic syndrome; spending six or more years at facilities results in a risk of contracting chronic illnesses (Cole et al., 2000; Donham et al., 2007). On a larger scale, CAFOs affect its surrounding communities by similarly increasing the risk of developing respiratory illnesses, but also increasing the prevalence of blue baby syndrome and miscarriages for pregnant women through excess nitrate in water (Gregor et al., 2010). In addition to physical health, community members also suffer psychologically through experiencing a decreased quality of life—e.g. normal social activities impaired by noxious odors — resulting in a heightened prevalence of depression, fatigue, anger, and other related illness (Schiffman et al., 1995).

[3] A variety of particles that can react to form ozone

Although this paper is one of many existing works written on the broader environmental impacts of CAFOs, as far as I can tell, it is the first that specifically concentrates on China. Many researchers have analyzed the health impacts of CAFOs on humans. Others have considered particular pollutants present in waterways, but the main focus of this paper is through a wider lens. This paper looks at overall trends within the Chinese livestock sector and seeks to explore whether there is an association between the concentration of pollutants and the amount of livestock production in a given geographical area. This paper adds to the existing body of research on this topic and focuses on very specific variables, such as the total amount of nitrogen and phosphorus in wastewater and the livestock production index compiled by the World Bank.

Empirical Methodology

To evaluate the externalities caused by CAFOs, the method of combining sets of external secondary data published by the National Bureau of Statistics of China (NBS) and the World Bank (WB) was utilized. Both of these databases are publicly available and show an array of indices under different categories which serve as indicators of national wellbeing.

The National Bureau of Statistics of China offers different types of data: monthly, quarterly, annual, census, and other. Annual data was chosen because it is the easiest to manage and can be utilized to illustrate trends across the livestock industry; further, seasonal variations are easier to remove. Data was obtained from section 6: People's Living Conditions; section 8: Resources and Environment; and section 12: Agriculture. These sections were selected as they focus on the indicators most relevant to this study. Additionally, they show national comparisons across provinces and time.

The WB offers data across countries and compiles them from official international organizations as well as national databases. The data used focuses on China and specifically on pollutant emissions relating to the agricultural industry. Unlike NBS, the WB does not provide regional data but does offer access to a longer time frame (1970 to 2018). Therefore, this database was utilized more to illustrate long-term trends between specific indicators and their correlation.

Since data from NBS shows regional differences, the NBS database was utilized to show the correlation between pollutants in different regions as related to the prevalence of livestock produced.

Data and results

As an introduction to the empirical findings, Figure 1 and Table 1 present differences in meat production for four geographical regions: Shanghai, Jiangxi, Hunan, and Shandong. These regions were chosen as Shanghai produces the least amount of meat in China, and Shandong produces among the most. Differences in meat production in the four regions are analyzed to see the relationship between the amount of meat production and the amount of nutrients present. Table 1 presents data on the production of meat and nitrogen and phosphorous emissions for the four regions in the year 2017.

Figure 1
Meat production and pollutants in wastewater in selected regions, 2017

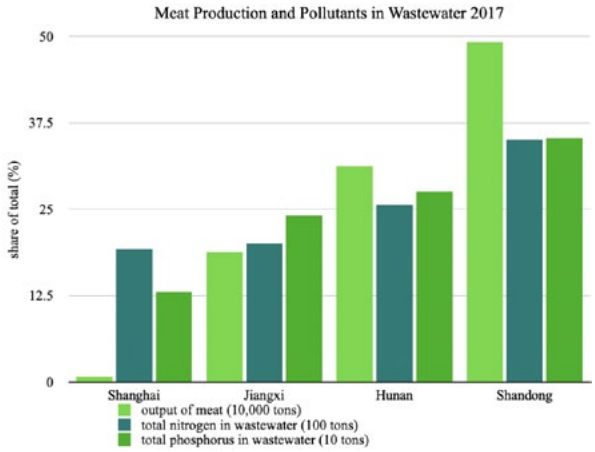

Note. Data obtained from the National Bureau of Statistics, http://data.stats.gov.cn/index.

Table 1
Meat production and pollutants in wastewater, 2017

Baseline indicators	Shanghai	Jiangxi	Hunan	Shandong
Output of meat (10,000 tons)	17.4	330.9	529.8	777.5
Total nitrogen in waste water (10,000 tons)	7.76	8.08	10.33	14.14
Total phosphorus in waste water (10,000 tons)	0.27	0.50	0.57	0.73

Note. Data obtained from the National Bureau of Statistics, http://data.stats.gov.cn/index.

As is evident in Figure 1, Shanghai produces the least amount of meat and Shandong produces the most. Jiangxi and Hunan are somewhere in between. The variables highlighted in the figure are output of meat, total nitrogen in wastewater, and total phosphorus in wastewater. The latter two variables represent the main pollutants in water associated with meat production. Though Shanghai produces the least meat, its wastewater pollution levels remain relatively high. This is due to the comparatively smaller surface area of the region, which leads to a concentration of the nutrients accumulating in bodies of water.

Figure 1 and Table 1 illustrate the output of meat in four regions along with two of the most common pollutants resulting from animal manure and fertilizer application: nitrogen and phosphorous. The data in Figure 1 is represented as a share of total output and total emissions, while Table 1 provides the actual total values. As can be observed, there is a positive correlation between the output of meat and the number of pollutants emitted. It is shown that in these four regions in 2017, regions with a higher output of meat also had higher total nitrogen and total phosphorus in wastewater.

Nitrogen ends up in the atmosphere mainly due to agricultural processes, such as soil erosion and manure management. However, there could also be other factors that influence its presence, such as fossil fuel emissions from vehicles. The correlation between the output of meat with total nitrogen and output of meat with total phosphorus is very high, 0.936 and 0.989 respectively. Despite this, Shanghai is an anomaly. Even though its output of meat is significantly lower than the other three provinces, the concentration of total nitrogen and phosphorus in wastewater remains relatively high due to its small surface area.

Table 2
Population in four regions, 2017

Baseline indicators	Shanghai	Jiangxi	Hunan	Shandong
Population (10,000 persons)	2418	4622	6860	10006
Population Density (inhabitants per square kilometer)	3814	276.9	323.8	634.5

Note. Data obtained from the National Bureau of

Statistics, http://data.stats.gov.cn/index, and Statista, https://www.statista.com/.

Table 2 introduces another factor that may explain the different levels of pollutants present: is population density. Both nitrogen and phosphorus have a negative correlation coefficient with it, -0.447 for nitrogen in wastewater, and -0.814 for phosphorus in wastewater, which may indicate that population density may not be the only factor generating these pollutants.

Additionally, the correlation between total nitrogen and total phosphorus in all the regions is +0.88, showing that in 2017, regions with higher total nitrogen in wastewater also had higher total phosphorus. This would make sense as both pollutants are present in livestock production from fertilizer and animal manure. The high correlation could indicate that livestock production is one of the main sources of both pollutants, as this industry is one of the only ones that emit both.

Figure 2 and Table 3 illustrate the output of meat in the same four regions along with nitrogen oxides (released during the treatment and storing of livestock manure), and smoke and dust (released through ventilation of animal houses).

Figure 2
Meat production and pollutants in waste gas in selected regions, 2017

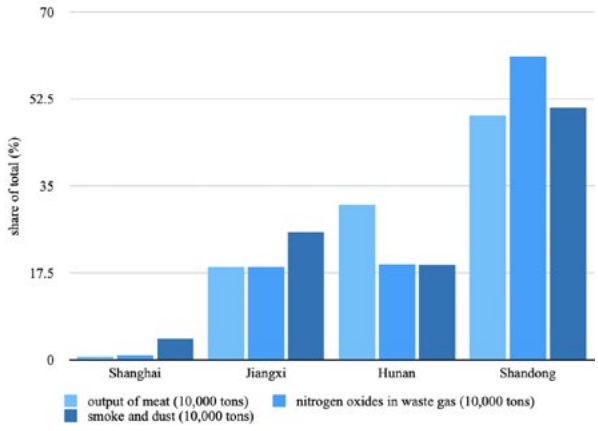

Note. Data obtained from the National Bureau of Statistics, http://data.stats.gov.cn/index.

Table 3
Meat production and pollutants in waste gas, 2017

Baseline indicators	Shanghai	Jiangxi	Hunan	Shandong
Output of meat (10,000 tons)	17.4	330.9	529.8	777.5
Nitrogen oxides in waste gas (10,000 tons)	19.39	35.54	36.47	115.86
Smoke and dust in waste gas (10,000 tons)	4.70	27.95	20.71	54.96

Note. Data obtained from the National Bureau of Statistics, http://data.stats.gov.cn/index.

As the data in Figure 2 and Table 3 shows, out of the four regions in 2017, regions with a higher output of meat also have higher nitrogen oxides. The same is true for smoke and dust in three of the four regions, with Hunan being the exception. It is interesting to note that the correlation between the output of meat with smoke and dust (+0.913) is higher than the correlation between the output of meat with nitrogen oxides (+0.881). This remains the case even after taking into consideration the dip in Hunan.

In Hunan, the differences in the composition of gross domestic product (GDP) may account for the departure from the direct positive association between the output of meat and smoke and dust. Although both pollutants, nitrogen oxides and smoke and dust, are emitted through the livestock sector, the main contributors to nitrogen oxides and particular matter are combustion processes from automobiles and other industries (ScienceDirect, 2021). GDP is made up of primary, secondary, and tertiary industries. Primary industry concerns harvesting raw materials, which includes agriculture, mining, and forestry. Secondary industry, also known as the manufacturing sector, converts the materials obtained from primary industry into consumer products. Out of the four regions, Jiangxi has the highest concentration on the secondary industry, 46.6 percent, compared to Shandong's 39.8 percent, Hunan's 37.6 percent, and Shanghai's 27 percent. Therefore, Hunan's comparatively lower focus on the secondary industry may explain the smaller amount of pollutants in the waste gas, as the secondary industry is the main contributor to the prevalence of these pollutants.

Additionally, the amount of pollutants emitted in Shanghai is unusually low compared with the other three regions, which could be explained by this city's more developed state. As China's main metropolis, it has more access to innovative and greener technology and is more conscientious of the air quality that its citizens breathe. Therefore, it is unsurprising that it also has the least amount of pollutants.

When the data is compared to population density in Table 2, there is a negative correlation between the presence of pollutants in waste gas and population density: -0.416 for nitrogen oxides and -0.646 for smoke and dust. This may indicate that the amount of inhabitants per square kilometer is not necessarily the only factor that explains the presence of pollutants. As data regarding meat production and water-gas pollutants indicates, when the output of meat increases in 2017, so does nitrogen oxides and smoke and dust in waste gas.

Table 4
Livestock production index and greenhouse gas emissions

Baseline indicators	2006	2007	2008	2009	2010	2011	2012
Livestock production index (2014-2016=100)	84.07	84.14	88.23	91.3	93.59	94.05	97.38
Total greenhouse gas emissions (% change from 1990)	120.24	134.39	157.46	172.75	187.30	209.92	219.95

Note. Data obtained from the World Bank, data.worldbank.org.

Table 4 displays data compiled from the World Bank's livestock production index and total greenhouse gas emissions as a percentage change from 1990 in China. The livestock production index is an aggregate of livestock production compared to the base period 2014-2016. It is calculated through the Laspeyres formula and compiled by the Food and Agricultural Organization of the United Nations (FAO).

When examined, the correlation coefficient between the two variables, livestock production index and total greenhouse gas emissions, is nearly perfect, +0.98 (p-value = 0.00012). The correlation is statistically significant, showing that from 2006-2012, as livestock production increased, the amount of total greenhouse gas emissions also increased. This conclusion is further supported in earlier findings (figure 2, table 3) where the prevalence of nitrogen oxides and smoke and dust exhibit a high positive correlation with the output of meat. Other greenhouse gases emitted from livestock production would include methane, primarily from cattle digestive processes (Grossi et al., 2019). In all, the strong positive correlation between the livestock production index and greenhouse gas emissions, which encompasses nitrogen oxides and smoke and dust, indicates that livestock processes might be one of the main contributors to rising greenhouse gas emissions.

Conclusions and policy recommendations

To analyze the negative externalities arising from CAFO production in China, I compared four geographical regions differing in the output of meat with pollutants: nitrogen in wastewater, phosphorus in wastewater, nitrogen oxides in the waste gas, and smoke and dust in waste gas. All four pollutants showed a high positive correlation with the output of meat. Additionally, there is a strong positive correlation between the livestock production index and the amount of greenhouse gas emissions.

The trend of converting to large-scale factory farms in China in the last few decades has been well documented. Therefore, it is reasonable to assume that the high output of meat is an indication of the existence of CAFO factories in different geographical areas. Though it may not be the only reason, it is certainly plausible to assume that livestock, and effectively, CAFOs, contribute to the varying pollutant levels found throughout the country.

A policy recommendation that emanates from my findings is that access to greener technology may help dampen pollution levels. This is most apparent in Shanghai, which is by far, the least polluted region out of the four regions analyzed here. As the most technologically advanced city, it makes sense that there is greater emphasis placed on environmental standards, and more research to improve living conditions. With this added innovation, it can be assumed that greener technology is one of the facets leading to its overall less polluted climate.

Exploration of CGAN Pix2Pix Model with Image Data for S&P Stock Price Prediction

By Cindy Su

Author Bio

Cindy is a high school junior at Phillips Exeter Academy in Exeter, New Hampshire. She is interested in education technology, business, and the usage of artificial intelligence in our society. She is a self-starter and entrepreneur, her most recent project being the co-founder and Curriculum Director for the DreamAI, an organization intended to introduce AI and its various applications to middle schoolers. She is a constant learner of coding and computer science, picking up Java on her own through Khan Academy and studying Python through various elective classes at her school and summer programs such as AI4ALL. Currently, she is working on Speciify, a business and app aiming to help special educators better organize their classrooms and manage their students.

Abstract

With the incredibly volatile stock market in 2020, many professional investors won big, but almost all average citizen investors lacked the resources to participate, such as investment knowledge, time, attention, and buying capital,, leaving them at a great disadvantage. There have been AI and prediction algorithms that have been developed that are making “smart” investing available to more people, but the algorithms are still difficult to understand as there is a code language barrier. The algorithms are also difficult to trust as they are opaque in how they process strictly numerical data into predictions. Thus, this experiment tested to see if an image data-based algorithm like the Pix2Pix Conditional Generative Adversarial Network (CGAN) would be able to predict the next week’s stock prices. By focusing on image data, it promotes more understanding of the algorithm as common investors can more easily see patterns through visual representations of stock prices. It also explores the Gramian Angular Summation/Difference Fields (GAF) image representation method that could encode more pertinent relationships between data points than a direct candlestick image. Experiments ended up showing that the model’s prediction GAF image for the next week’s prices had a 74% similarity rate with the GAF image of the next week’s actual prices, suggesting that the image-based model and GAFs could be considered for future stock prediction.

Keywords: Generative Adversarial Networks, Stock Market, Time-Series, Optimization, Prediction, Artificial Intelligence, Gramian Angular Fields, Image Data, CGAN, Candlestick Graphs

Introduction

Millions of Americans with money staked in the stock market lose precious savings in the stock market every day. In fact, more than 50% of all US families own publicly traded stock in some form, often drawn in by promises of money and fortune (1). The COVID-19 pandemic has only increased public interest in the stock market, especially with Congress representatives making more than $290 million through trading in 2020 (2). However, most of the time, investments in the stock market made by common citizens lose money, with over $415 billion lost in 2020 as they do not have the same access to resources and knowledge as professional investors (3). Thus, this research aims to address how technology may be able to help more citizens win in the stock market, the computer algorithm acting as a stock market "advisor" by predicting the next week's stock prices. This isn't a new concept, as there are already existing AI models that operate by predicting future events through the analysis of historical data and trends. The most common method used to predict stock price change is based on LSTM (Long Short-Term Memory), a deep learning framework for time-series, to build a predictive model (4, 5). This method uses numerical stock values (open, close, and high, low, and volume) directly to train the models (6). Although this method has seen success so far, it is impossible for a human to look at the same numerical data and process the information immediately and draw useful conclusions (7). If the algorithm used visual data, particularly starting with graphs that humans can easily read, it could increase the trust and transparency of these predictive model to the average consumer. Therefore, we also wanted to focus on trying to use image data in our stock prediction algorithm so it would be easier to understand from an untrained eye. We turned towards Generative Adversarial Networks to create an understandable and accurate model.

Generative Adversarial Networks, or GANs, are a class of machine learning frameworks designed by Ian Goodfellow in June 2014 (8). The adversarial process involves using two neural networks that compete against each other in a zero-sum game; the generator tries to create similar images from an existing data set that will confuse the other network, the discriminator, into classifying the generated images as real data. Since the "indirect" training happens through the discriminator, it also updates itself and the generator constantly, allowing the model to learn in an unsupervised manner. This powerful architecture has researched in the past for stock prediction, using networks like Multi-Layer Perception (MLP) and LSTM, and showed promising results that show the potential of image-based prediction (9). Specifically, the Pix2Pix CGAN, typically used for image-to-image translation, works off of the previous data entered. Thus, the conditional aspect of the network ensures that the newly generated image is a time-series prediction, not just a random candlestick graph, hypothetically making the predicted images more accurate. The Pix2Pix CGAN is unique in the way that it does not use the popular LSTM algorithm and instead uses a generator with a U-Net-based architecture and a discriminator represented by a convolutional PatchCGAN classifier (10). U-Net is an architecture for semantic segmentation. PatchCGAN is a type of discriminator that runs convolutionally across the image, trying to classify if each patch in an image is real or fake, and then averaging all responses to provide the ultimate decision

We hypothesized that image data and the Pix2Pix CGAN model would be able to predict stock prices, and conducted two main experiments, which will be referenced throughout this paper. Both experiments were meant as an iterative experimental process to further discover the potential and use of CGANs in time series prediction. The main difference between the two experiments is the type of data that was used. The same stock market index was used, the Standard and Poor's 500, otherwise known as SPY, because it gives a general sense of how the market is doing and the specific stock is not particularly important as we are testing the overall effectiveness of the prediction method. For the first experiment, I used images of candlestick graphs from 1993 to 2003, but in the second experiment, we used more recent data spanning from 2009 to 2019 and eliminated the graph formatting distractions by directly encoding the numbers into GAF images. Candlestick charts cleanly display the open, high, low, and close of the day, and are easy to interpret at a glance, making them our first choice as image data to train the CGAN on. However, because the stock market's prices have such a large range over each 10-year period, the candlestick charts automatically scale themselves to display each week's candles most optimally (Fig. 1). This raises the

problem of standardizing each image's scale, which is incredibly difficult to do as many of the smaller candlesticks become invisible when the scale becomes too big. After reading about Gramian Angular Fields (GAFs), which represent numerical time-series data in a non-Cartesian coordinates system, we realized it would eliminate the issue of scaling for all pieces of data (11). The black and white encoded images do lose transparency for the general reader of the data images (Fig. 2). Nonetheless, using the GAF package is a clean way to ensure all images are equal (5x5 pixels) and can speak to the promise of time-series prediction using image-based data (12, 13). After both experiments, we saw that our results supported our hypothesis: the conditional generative adversarial network was able to use image data to predict the price of the S&P 500 with relative accuracy.

Results

In the first experiment, images of candlestick graphs of SPY data from 1993 to 2003 were analysed to see if the Pix2Pix CGAN on Google Colabratory could be used to predict the next week's stocks. Unfortunately, we were unable to come up with conclusive results as the generated images looked completely different from the real graphs. They could also not be interpreted because each candlestick would have multiple ending points and spindles, which indicate the prices at which the stock closes and opens at, crucial to determining a prediction for the next day. However, all the fake images were able to pick up the general candlestick shape, with a rectangle and spindles sticking out on the ends, as well as the separation between the five candlesticks, which can speak to the effectiveness of the CGAN itself (Fig. 3).

In the second experiment, GAFs were analyzed to encode the highest price that the S&P 500 hit each day from 2009 to 2019. We also wanted to quantify our results and accuracy of the method, so we decided to use a cosine similarity function to determine the similarity between the fake images that were generated as predictions and the real images that were used as tests (Fig. 4). After calculating the similarity percentage of each pair of images using a pixel-by-pixel comparison, we got a final average of 0.7383, or around a 74% similarity rate of the entire model.

Discussion

When analyzing our first experiment, it was identified that there were some fundamental things amiss with the images we trained the Pix2Pix CGAN on, so it wasn't unexpected that we didn't have clear and conclusive answers. The CGAN was unable to pick up the significance of white and black candlesticks, which represented bullish and bearish patterns, and tended to make all the generated images white candlesticks. There were also often many spindles and cutoff points on one candlestick, which was inaccurate and didn't provide any actual interpretable value. One of the most fundamental problems with these graphs in experiment 1 is that the images included the axis numbers, axis titles, and white space around each image. The axis labels were unreadable and only added noise to the image. A deeper problem discovered was that the images did not have the same scaling for each photo, which meant some photos would display more range of monetary value than others. In the second experiment, although an average of 74% accuracy may not seem very high, if we consider the context of CGANs as well as the danger of overfitting, this proves that the CGAN model has great potential in being used as a trustworthy way to predict stock market data.

There are benefits and drawbacks of both types of usage of the CGAN model proposed. The model that uses the candlestick graphs makes the data easier to understand for the public eye, but they are more difficult to train with because they have more components within the image the CGAN needs to filter out and account for when trying to make a prediction. The second method with the GAF images is harder to understand, but it can streamline the process of training the CGAN and prediction, which would likely provide more accurate results.

There are two novel things about the research completed in this paper: the usage of image rather than raw numerical data, and the encoding of time-series data using GAFs. The goal of exploring and implementing this new method of predicting stocks is to increase awareness and promote more engagement with this intersection of financial and AI literacy. Future work could involve a series of "mix and matches". This means changing variables such as the kind of GAN used (implementing LSTM, MLP, or

other networks), the specific stock or index used, using a different data point out of the OHLC of a stock, running multiple experiments with OHLC and then evaluating all of them together to get a better overall sense of the stock, etc. (14). We believe there is a point where these two approaches explored in our research can come together so that not only can we include visual data to increase transparency with consumers, but also preserve the accuracy rate achieved when using GAFs (15). This method could be applicable to different kinds of time-series datasets and can be further developed so that the model is easier for the public to use, adapt to, and understand.

Materials And Methods

Experiment 1: Candlestick Graphs

In the first experiment, I used SPY (SPDR S&P 500 trust) data from 2/22/1993 to 4/17/2003, 10 years, to create 512 images in total. Each image featured 5 candlesticks on one graph since each candlestick represents one day, the entire image represents one week of trading. In addition, each image is at the size of 800 x 575 pixels, including the extra margin of white space. Each graph is lined with a black outline, with axis labels including the written month and date. The background of the graph is the same for each one, a light blue with white lines, and each candlestick is of the same width, though they are either black or white depending on if the stock fell or rose from its opening price that day, respectively (Fig. 1). They also have needles on each side of each candlestick as it represents the range the price hit that day.

Experiment 2: GAF Images

In the second experiment, the data was shifted to be more recent SPY data in a time range from 01/02/2009 to 12/30/2019, 10 years with 552 images in total. This time frame was chosen because it avoids any extremely dramatic movements in the overall market. The data starts by recovering from the 2008 recession and ends right before the COVID-19 pandemic, which resulted in drastic aftereffects, including the huge crash in March of 2020. Considering the goal of this experiment was to test the effectiveness of the image prediction method, this particular time frame avoided potentially "confusing" the CGAN with such dramatic stock differences in short amounts of time, as they were "black swan" events and don't accurately represent what the algorithm would be predicting if applied to the real world.

The most important difference in the second experiment was that the use of Gramian Angular Fields, or GAFs, was implemented.. My original reason to choose GAFs is that it was difficult to manipulate the graphs do not include the white margins and different words on the axis changes a numerical data point to a pixel, it can only do one numerical data point at a time, so the high data point was chosen since we were curious about possible predicting the "potential" of a stock. However, after studying the mathematics meaning of GAFs, it was concluded that a GAFs image provides more pertinent information of the times series data: GAFs essentially are relationships between every point and every other point in the time series. It also allows for the exploration of a more effective image-based presentation than a traditional candlestick chart for time series data.

To turn the numerical stock data into images, I used two slightly different methods for the two experiments. In the first experiment, I used the Python package Matplotlib Finance to create candlestick graphs from the numerical data. I looped through all the data in 5-day increments and saved them to my Drive through a mounted folder on Google Colab. In the second experiment, I followed the same steps, only creating GAF images using the code package from the Chen and Tsai experiment. Then, I split my image data in both experiments into A and B sets, with subsections of training and testing sets. For experiment 1, I split the 512 images into two folders- A and B. 256 images went into each, and within each A and B folder were 51 images placed into testing and 205 in the training folder that met a 20/80 split, respectively. Folder A contained the first week and every other week's (even weeks) data after that, while the B folder included the second week and every other week's (odd weeks) data afterward. This allowed for the Pix2Pix CGAN to place every two weeks' images together and hypothetically find a correlation from one week to the next. In the second experiment, I followed the same steps, the only difference being that there were 552 GAF images in total, with 276 in A and B each and 54 test and 222 training images, maintaining the 20/80 split from the first experiment.

Acknowledgements

To Dr. Ganesh Mani at the Institute for Software Research in Carnegie Mellon University, thank you so much for your constant guidance and support. Thanks to Grace Su, Computer Science Student and AI Researcher at Columbia University, who provided me with initial research feedback and coding guidance.

References

1. Federal Reserve. (2021, March 2). USA Facts. https://usafacts.org/articles/what-percentage-of-americans-own-stock/

2. Unusual Whales. (2022, January 10). Congressional trading in 2021. Unusual Whales. https://unusualwhales.com/i_am_the_senate/full

3. Dream Exchange. (2021, March 12). Cision PR Newswire. https://www.prnewswire.com/news-releases/3-financial-literacy-statistics-that-need-to-change-in-2021-301246352.html

4. Loukas, S. (2020, July 10). Time-Series forecasting: Predicting stock prices using an LSTM model. Towards Data Science. https://towardsdatascience.com/lstm-time-series-forecasting-predicting-stock-prices-using-an-lstm-model-6223e9644a2f

5. P, S. (2021, May 19). Stock price prediction and forecasting using stacked LSTM. Analytics Vidhya. https://www.analyticsvidhya.com/blog/2021/05/stock-price-prediction-and-forecasting-using-stacked-lstm/

6. Kumar, V. (2020, March 27). Hands-On guide to LSTM recurrent neural network for stock market prediction. Analytics India Magazine. https://analyticsindiamag.com/hands-on-guide-to-lstm-recurrent-neural-network-for-stock-market-prediction/

7. Lee, Y. H. (2021, February 16). Analysis of stock price predictions using LSTM models. Analytics Vidhya. https://medium.com/analytics-vidhya/analysis-of-stock-price-predictions-using-lstm-models-f993faa524c4

8. Goodfellow, I., Pouget-abadie, J., Mirza, M., Xu, B., Warde-farley, D., Ozair, S., Courville, A., & Bengio, Y. (2020). Generative adversarial networks. Communications of the ACM, 63(11), 139-144. https://doi.org/10.1145/3422622

9. Zhang, K., Zhong, G., Dong, J., Wang, S., & Wang, Y. (2019). Stock market prediction based on generative adversarial network [Paper presentation]. International Conference on Identification, Information and Knowledge in the Internet of Things. https://www.sciencedirect.com/science/article/pii/S1877050919302789

10. Isola, P., Zhu, J.-Y., Zhou, T., & Efros, A. A. (n.d.). Image-to-Image translation with conditional adversarial networks. arXiv. https://doi.org/10.48550/arXiv.1611.07004

11. Chen, J.-H., & Tsai, Y.-C. (2020). Encoding candlesticks as images for pattern classification using convolutional neural networks. Financial Innovation, 6(1). https://doi.org/10.1186/s40854-020-00187-0

12. Mazzoni, C. (2021, February 19). How to encode time-series into images for financial forecasting using convolutional neural networks. Towards Data Science. https://www.google.com/url?q=https://towardsdatascience.com/how-to-encode-time-series-into-images-for-financial-forecasting-using-convolutional-neural-networks-5683eb5c53d9&sa=D&source=docs&ust=1640962878l-286&usg=AOvVaw1IxgRloBawDANaJeaV2vEV

13. de Vitry, L. (2018, October 14). Encoding time series as images gramian angular field imaging. Analytics Vidhya. https://medium.com/analytics-vidhya/encoding-time-series-as-images-b043becbdbf3#:~:text=Gramian%20Angular%20Field%20Imaging%20%7C%20by,de%20Vitry%20%7C%20Analytics%20Vidhya%20%7C%20Medium

14. Ganegedara, T. (2020, January 1). Stock market predictions with LSTM in python. Datacamp. https://www.datacamp.com/community/tutorials/lstm-python-stock-market

15. Wang, Z., & Oates, T. (n.d.). Imaging time-series to improve classification and imputation. ArXiv. org. https://arxiv.org/pdf/1506.00327.pdf

Figures and Figure Captions

Figure 1. Image #430 from the training data of Set A in Experiment 1. 5 candlesticks are displayed with 3 white (bullish) and 2 black (bearish) candles. Created using Matplotlib graphs in Google Colaboratory.

Figure 2. Real GAF image #442 from the training data of Set A in Experiment 2. Originally 5 by 5 pixels, it is a blown up black and white image, and was created in Google Colabratory using the GAF package from the original "Encoding Candlesticks as Images" paper (8).

Figure 3. Fake Generated Image #2270 in Experiment 1. There are 5 white rectangles on a light blue square background, which was generated by the Pix2Pix CGAN in Google Colabratory as the next week prediction of stock prices.

Figure 4. Screenshot of my code in Google Colabratory of the cosine similarity function I used to calculate the accuracy rate displayed on the last line of output.

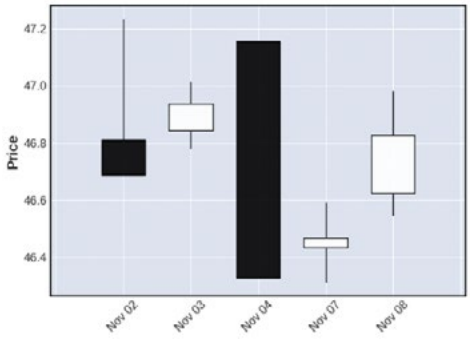

Figure 1

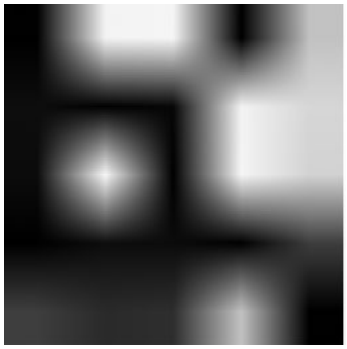

Figure 2

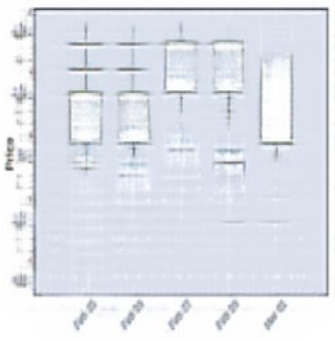

Figure 3

```
[ ]  1 sim_list = []
     2 for i in range(444, 543, 2):
     3   img1 = plt.imread('/content/drive/MyDrive/Academic Mentor- Ganesh Mani/images_exp2/B/test/pytorch-CycleGAN-and-pix2pix/results/stocks_pix2pix/test_late
     4   img2 = plt.imread('/content/drive/MyDrive/Academic Mentor- Ganesh Mani/images_exp2/B/test/pytorch-CycleGAN-and-pix2pix/results/stocks_pix2pix/test_late
     5   img1 = torch.tensor(img1)
     6   img2 = torch.tensor(img2)
     7   output = F.cosine_similarity(img1, img2, dim=1)
     8   overall = torch.mean(output, dim=(0,1))
     9   sim_list.append(overall)

[ ]  1 print(sim_list)

     [tensor(0.6809), tensor(0.6411), tensor(0.7790), tensor(0.8149), tensor(0.7688), tensor(0.8781), tensor(0.7633), tensor(0.8677), tensor(0.8527), tensor(0.629

[ ]  1 print(sum(sim_list) / len(sim_list))

     tensor(0.7383)
```

Figure 4

Application of Machine Learning in Predicting Molecular Properties

By Edward Sun

Author Bio

Edward Sun is currently a high school junior attending Union County Magnet High School in Scotch Plains, New Jersey. He is, and has been, a National Chemistry Olympiad Finalist in 2022 and 2021, and has participated in the North Jersey Regional Science Fair, hosted by Nokia Bell Labs. Ever since he was a child, he was fascinated by chemistry, and in middle school, took an interest in computer science as well, and sought to find a way to unite the two subjects. In this paper, he utilizes machine learning algorithms to predict the melting points of organic compounds from their structures, and hopes that this research will build a foundation for many revolutionary steps to come in utilizing machine learning in diverse scientific subjects, ranging from medicine to astronomy.

Abstract

As developing new compounds and determining their properties is expensive and possibly dangerous, it becomes necessary to develop a model to predict the molecular properties without having to synthesize and test it experimentally. Two systematic ways to represent a compound are through the schematic diagram of the molecular structure and the simplified molecular-input line-entry system (SMILES). In this study, these representations were used to train two neural network models, a convolutional neural network (CNN) and a recurrent neural network (RNN), respectively, in order to predict the compounds' melting points. By representing the compounds as an image of the structure, the CNN was unsuccessful at fitting the given data, appearing to remain constant at around the average melting point of the given data. However, by representing the compounds as a systematically generated string of text, the RNN was successful at fitting the data, with an overall trend similar to the actual trend and a lower mean absolute error. However, the SMILES data used for the RNN does not contain orientation information, unlike the structure diagram data. For future studies, it may be possible to combine the two representations to reach a more accurate prediction model.

Keywords: Chemistry, computational, machine learning, molecular properties, neural network, convolutional, recurrent

Background

Chemistry is the science that deals with the properties, composition, and structures of substances, and how they transform into other substances. Therefore, it is one of the most useful fields for medicine by synthesizing new compounds as novel drugs. To effectively synthesize stable and reliable chemicals for medical treatment, it is important that the physicochemical properties of specific organic compounds can be determined in order to infer its use as a drug, such as solubility, membrane permeability, or stability (Mi et al., 2021). However, determining these properties can be both dangerous and costly. Specifically, it is inefficient and expensive to measure all the necessary properties of every organic compound in order to quantify its use as a drug. For example, determining properties like the precise melting point of a compound is difficult to do with a huge number of these compounds. In addition, some of these experiments can be hazardous or dangerous to the experimentalist. Thus, it becomes necessary to develop a model to predict such properties with relative accuracy without using experimental methods.

With the rise of machine learning, neural networks are becoming an increasingly popular model to predict various properties, including chemical properties (Salahinejad et al., 2013). While it is easy for a human to determine, for instance, around what range a compound's melting point is based only on its structure, it is far more difficult to get an accurate number for the melting point from the structure only. It is possible that machine learning could achieve similar or superior predictions on the melting point compared to human prediction. By analyzing the structure in a complex mathematical form, a neural network can take in the structure of a compound and output a number for the melting point. Despite the challenges to understand how the neural network calculates the melting point explicitly, the mechanism behind the learning process is nevertheless generally understood.

Previous research (Mi et al., 2021) has attempted to predict melting points using the simplified molecular-input line-entry system (SMILES) with various machine learning models. The SMILES system has the advantage over the actual structure schematic of being a single line of text; however, it does not contain complete information on the orientation, which could also affect the melting point. However, no studies have been performed using orientation information to predict melting point. Therefore, the objective of this study is to develop a machine learning model to predict melting point of chemicals and to investigate whether orientation information affects the melting point.

Method

In this study, Google Collab was used to run all the programs, using the built-in neural network foundation TensorFlow, interfacing with the Python 3 programming language with the Keras library.

First, the dataset of compound names, their SMILES data, and their melting points were obtained and extracted into a list (Bradley et al., 2019). Then, each entry of the list was formatted such that all SMILES text was converted into an array of numbers, with each number representing a unique letter of the text. Also, images of the structures were extracted from PubChem using an automated scraper and compiled separately Then, the list of formatted data was divided into training and validation inputs and outputs, with 20% of the original data being used for validation.

Afterward, the neural network architecture was constructed using Keras. Two models were used for this project: a bidirectional recurrent neural network and a convolutional neural network. For the first RNN, the first layer was an embedding layer, converting the indices of the inputs into dense vectors. The second and third layers were both bidirectional LSTM layers, and the final layer was a dense layer with only one node as the output. For the second CNN, an input layer of a 128 x 128 image was used, with the input images being converted into grayscale and rescaled to be a two dimensional tensor with values between 0 and 1. Then, two convolution and pooling layers were used, and then a flattening layer leading into three dense layers, with the final dense layer having only one node as output. In both, mean squared error was used as the loss function.

After all the data was collected, each network was trained for ten epochs, training on 90% of the original dataset and validating using the remaining 10%. After the models were fit, the loss values over time were plotted. Then, using a sample of 500

random inputs from the validation set, a scatterplot of melting point predictions were plotted, with the x-axis being the actual melting point and the y-axis being the predicted melting point. The scatterplot was compared to a straight line corresponding to the actual and predicted numbers being equal. To evaluate the accuracy of the models, the mean absolute error of the validation set in the final epoch of training was used, as well as the correlation coefficients of the scatterplots.

Results

The CNN model was not successful in predicting the melting point of chemicals. Specifically, it predicted almost no variance in the melting point compared to the actual data. The model does not seem to be sensitive to various predictors (Figure 1). The predicted melting point was consistently at 76.4 °C.

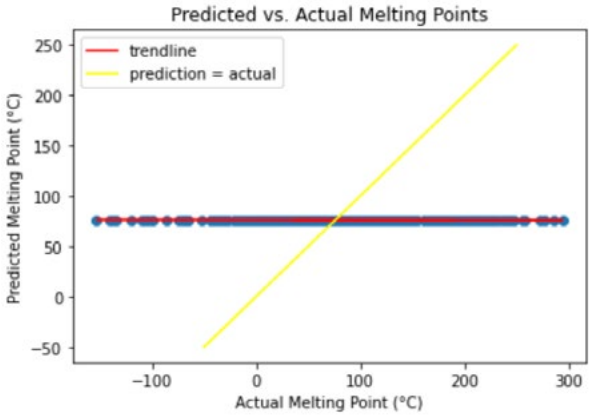

Figure 1. Predicted melting point against actual melting point from CNN. Each dot represents a prediction of one chemical. The yellow line represents when the prediction is equal to the actual value.

However, when zooming into the CNN graph (Figure 2), an opposite trend to the actual trend was observed. As the actual melting point increases, the predicted melting point slightly decreases instead, resulting in a negative correlation coefficient (Table 1).

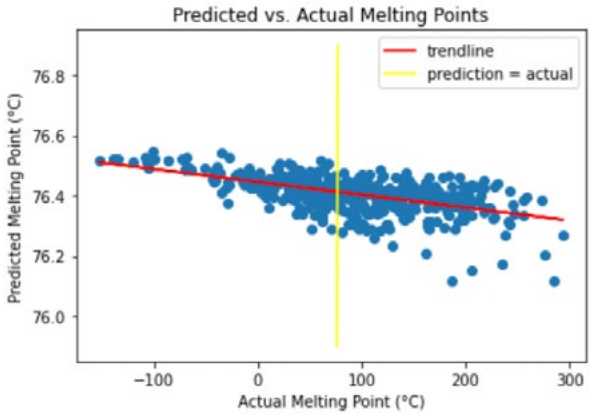

Figure 2. Zoomed in graph from Fig. 1 concentrated on predictions to show the slight downward trend of CNN predictions.

Compared to the CNN, predicted melting points by the RNN showed a higher sensitivity to various predictors and a higher variance. The overall trend is close to the actual trend, albeit with a less steep slope (Figure 3). The melting point predictions for the RNN appear to have a minimum of -50oC and a maximum of 204oC. Overall, the RNN showed a lower mean absolute error and a higher correlation coefficient than CNN (Table 1).

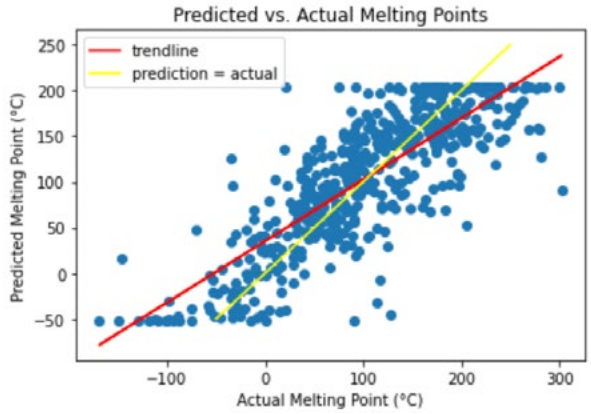

Figure 3. Predicted melting point against actual melting point from RNN. Each dot represents a prediction of one chemical.

Table 1. Correlation coefficient and mean absolute error of the two machine learning models.

Neural Network Type	Correlation Coefficient	Mean Absolute Error
Convolutional	-0.56775847	61.9855
Recurrent	0.81269509	38.5271

Discussion and Conclusion

Of the two neural network models, the recurrent neural network is better at prediction than the convolutional neural network. A possible explanation for the extremely poor performance of the CNN could be incorrect model design, such as inappropriate activation functions or loss functions. However, the dataset used may also be a contributing factor. The CNN used images of the compounds' structures as input, while the RNN used the SMILES data as input. The images used have a lot of empty space, which wastes a lot of computational power on the network on processing empty areas. Also, the scale of the molecule changes, since all images were originally in a 300 x 300 resolution, which could negatively affect the network's ability to recognise bonding structures.

The RNN is most likely useful for predicting melting points because of its ability to recognize sequences. Since organic compounds are typically made of functional groups attached to a long carbon chain, identifying these groups is extremely useful in determining the melting point. Another advantage of using the RNN is that it can recognize branches efficiently. Under the SMILES system, branches are enclosed in parentheses, which the RNN can interpret as a new branch. Since the RNN is primarily built for text processing, the SMILES system translates into regular text well, with parentheses acting like new "words" in the sentence.

Possibly a major factor contributing to the error in predictions for the RNN is the orientation information of the compound. SMILES cannot describe how a molecule is oriented, which makes it impossible to differentiate between stereoisomers such as diastereomers or enantiomers, even though this could have a large impact on the melting point of the compound. Another possibility is the limited data set; there was not enough data to form more accurate predictions. It is also unclear how the data from the original source was obtained, meaning there may be some sampling bias in the original dataset.

Future studies may use a more complex model for the predictions, as the current model does not contain that many neurons in order to save time and resources; a more complex model may be able to predict more accurately. Also, there are other molecular properties that can be predicted, such as boiling point, solubility, or heat of formation. With sufficient complexity, deep learning models may even be able to predict properties like toxicity or medical abilities by potentially finding previously unknown patterns in the structures of chemical compounds correlating to its effects on biological organisms. It may even be possible to reverse engineer the mechanism of a trained neural network by adjusting inputs and observing the changes in the output values, such as how effective a compound is in treating cancer. In conclusion, the most successful model of deep learning to predict molecular properties from the compound's structure, as was shown in this study, is a recurrent neural network trained using the SMILES format of text input.

References

1. Bradley, J.-C., Williams, A., & Lang, A. (2019, October 4). *Jean-Claude Bradley open melting point dataset*. figshare. Retrieved January 4, 2022, from https://figshare.com/articles/dataset/Jean_Claude_Bradley_Open_Melting_Point_Datset/1031637

2. Mi, W., Chen, H., Zhu, D. A., Zhang, T., & Qian, F. (2021). Melting point prediction of organic molecules by deciphering the chemical structure into a natural language. Chemical Communications, 57(21), 2633–2636.https://doi.org/10.1039/d0cc07384a

3. Salahinejad, M., Le, T. C., & Winkler, D. A. (2013). Capturing the crystal: Prediction of enthalpy of sublimation, crystal lattice energy, and melting points of organic compounds. *Journal of Chemical Information and Modeling*, 53(1), 223–229. https://doi.org/10.1021/ci3005012

Appendix

Below is some of the code that I used for the project

```
img_data = {}
err_names = []
print("[", end="")
for n in range(number_of_entries):
  if (n % (number_of_entries / 100) == 0):
    print("", end="")
  compound = list(data)[n]
  url = "https://pubchem.ncbi.nlm.nih.gov"
  d = "/rest/pug/compound/name/" + compound + "/PNG"
  response = requests.get(url + d)
  try:
    img = Image.open(BytesIO(response.content))
  except:
    err_names.append(list(data)[n])
    continue
  img = img.convert("L")
  img = img.resize((image_size, image_size))
  img = np.asarray(img)
  if len(img.shape) == 3:
    img = np.mean(img, axis=2)
  img_data[compound] = [img, data[compound]]
  sleep(0.1)
```

Code that iteratively obtains and processes images from PubChem for each compound in the dataset using the compound's conventional IUPAC name in the URL for PubChem's PUG-REST interface, for use in the CNN. First it assembles the URL, then after obtaining the image of the structure (printing errored requests if they occur), converts it into a Numpy array and inserts it into the global img_data dictionary that will serve as the input set for the network.

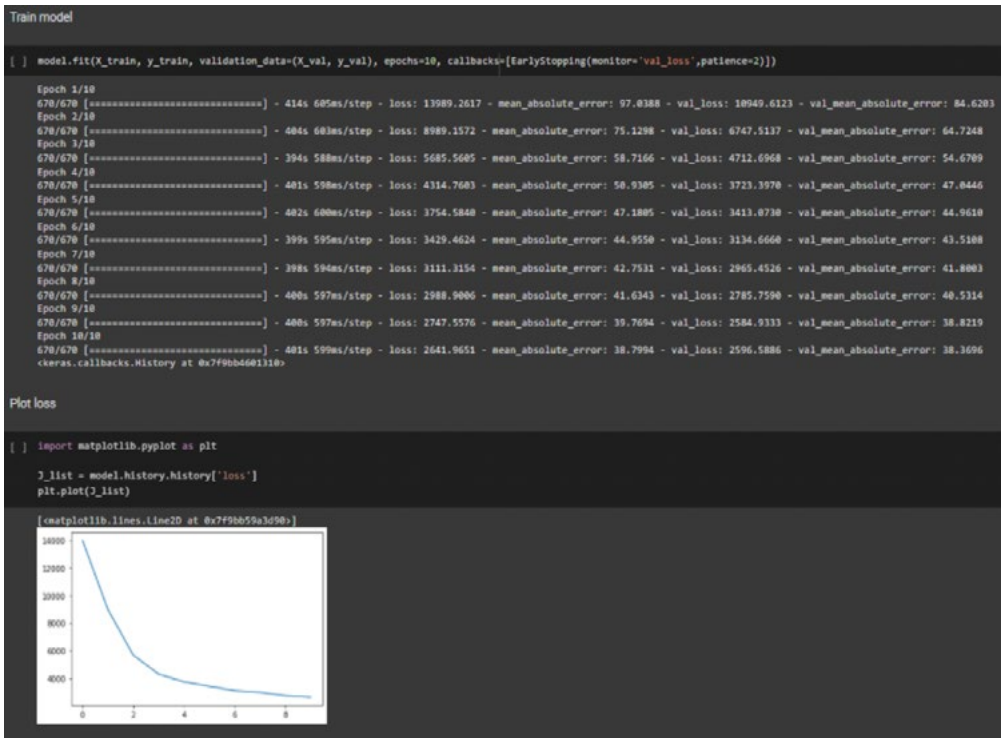

Appendix

Below is some of the code that I used for the project

```
img_data = {}
err_names = []
print("[", end="")
for n in range(number_of_entries):
  if (n % (number_of_entries / 100) == 0):
    print("▮", end="")
  compound = list(data)[n]
  url = "https://pubchem.ncbi.nlm.nih.gov"
  d = "/rest/pug/compound/name/" + compound + "/PNG"
  response = requests.get(url + d)
  try:
    img = Image.open(BytesIO(response.content))
  except:
    err_names.append(list(data)[n])
    continue
  img = img.convert("L")
  img = img.resize((image_size, image_size))
  img = np.asarray(img)
  if len(img.shape) == 3:
    img = np.mean(img, axis=2)
  img_data[compound] = [img, data[compound]]
  sleep(0.1)
```

Code that iteratively obtains and processes images from PubChem for each compound in the dataset using the compound's conventional IUPAC name in the URL for PubChem's PUG-REST interface, for use in the CNN. First it assembles the URL, then after obtaining the image of the structure (printing errored requests if they occur), converts it into a Numpy array and inserts it into the global img_data dictionary that will serve as the input set for the network.

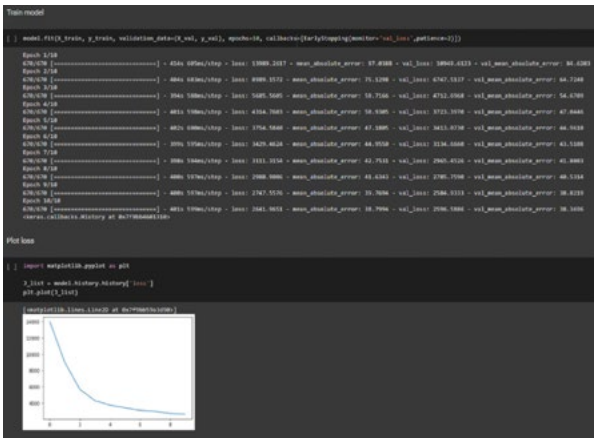

Top: Training output of RNN; for each epoch of training, the loss and mean absolute error are printed as each data entry is tested; after the training set for the epoch is completed, the validation subset is used on the network and printed to the right.
Bottom: plotted graph of loss value over time (mean squared error of melting point prediction) using Matplotlib. Loss decreases exponentially as the number of epochs increases.

```
rand_index = randint(0, len(X_val))
prediction = model.predict([X_val[rand_index]])
print("Name: " + name_smile[decode_smile_id(X_val[rand_index])])
print("SMILES: " + decode_smile_id(X_val[rand_index]))
print("Actual MP: " + str(data[decode_smile_id(X_val[rand_index])]))
print("Prediction: " + str(prediction[0][0]))
```

```
Name: (3beta,4alpha,5beta)-3,4-Dihydroxyandrostan-17-one
SMILES: O=C2[C@]1(CC[C@H]3[C@H]([C@@H]1CC2)CC[C@H]4[C@]3(C)CC[C@H](O)[C@H]4O)C
Actual MP: 221.0
Prediction: 184.39687
```

Random prediction from RNN, chooses random entry in the original dataset and feeds it into the network, then prints output.

Here, the selected compound is (3β,4α,5β)-3,4-dihydroxyandrostan-17-one, a steroid with a melting point of about 221.0°C. The melting point predicted by the RNN was about 184.4°C. The error in this instance is 36.6°C, close to the mean absolute error of the RNN.

```
predictions = []
print("Total possible predictions: " + str(len(X_val)))
print("Plotting: [", end="")
num_of_predictions = 500
for n in range(num_of_predictions):
  predictions.append(model.predict([X_val[n]])[0][0])
  if (n % (num_of_predictions / 100) == 0):
    print("▮", end="")
print("]")
predictions = np.array(predictions)
actuals = np.array(y_val[:num_of_predictions])


plt.scatter(actuals, predictions)
plt.xlabel("Actual Melting Point (°C)")
plt.ylabel("Predicted Melting Point (°C)")
m, b = np.polyfit(actuals, predictions, 1)
plt.plot(actuals, m * actuals + b, color="red", label="trendline")
plt.plot([-50, 250], [-50, 250], color="yellow", label="prediction = actual")
plt.title("Predicted vs. Actual Melting Points")
plt.legend()
```

Code to generate a scatterplot of 500 random predictions of both the CNN and RNN using Matplotlib. First it generates all its predictions, then it plots all the points using the predicted melting points as the y-axis and the actual melting points as the x-axis. Then, it generates a linear curve of best fit for the data, and plots this line, along with another line that represents y = x, i.e. when the prediction is equal to the actual value.

The Overemphasized Legacy of the Napoleonic Code

By Zilei (Stevenson) Li

Author Bio

Zilei (Stevenson) Li is currently a junior at Worcester Academy, MA. He is particularly interested in world languages, comparative politics, and legal studies. Stevenson grows up in Beijing, China but had visited more than 30 countries around the world. During his sojourns in foreign lands, he was always eager to explore the history of the nation. France and Eastern Europe particularly interested Stevenson, and he started learning French and Russian by himself since middle school. Last semester, Stevenson completed a big research project on the Russian Revolution and the succeeding civil war. He participated in National History Day Contest and won the second place in all-state competition and a special award for his creativity.

Abstract

When we discuss the legacies of Napoleon, it is inevitable to disregard his contribution to global jurisprudence: the French Civil Code of 1804. As Emperor, Napoleon proposed to enhance his military achievements with a comprehensive codification. Although he was not the precedent in doing so, it was him who created the paradigm of all codes that we now consider "modern." For decades, historians investigating the course of Napoleon's codification have developed a plausible explanation of its unparalleled significance in the world; that is, it extensively embodies the ideas of the radical French Revolution, which undermined feudal regimes and shaped modern society. However, this argument reflects a common tendency of glossing the Code by adding personal interpretations through modern lenses; it is neither objective nor inaccurate. The first part of this study is largely based on James Gordley's essay (1994) on the myths of Napoleon's codification. We will see that ideas expressed in the Code were not as novel to people in the nineteenth century as principles of the Revolution were, because many concepts were proposed by early French writers and framers of Roman law. In the second part of the study, we will investigate the relation between codification and the modern world. We will use Latin America as an instance to illustrate the limitations of the Code due to its relative antiquity. When we combine the conclusions of the two parts, it is plain that the legacy of Napoleon's Code is often overemphasized in the modern world.

Keywords: Codification, Napoleon, civil law, jurisprudence, Revolution, Roman law, legislation, equality, republicanism, property, contract, tort, case law

Introduction

"My true glory is not in having won forty battles; Waterloo will blot out the memory of those victories. But nothing can blot out my Civil Code. That will live eternally," Napoleon once said when he was in exile on Saint Helena (De Montholon, 1847, p.401). For centuries, historians and jurists have exalted the codification for its enshrinement of the great principles of the Revolution and the profound transformations it brought to the modern world. British barrister Maurice Amos comments: "Ever since the day of its promulgation France has done an enormous export trade in law; indeed, until the German Code was published, she was without a rival" (Amos, 1928, p.13).

So, what is this Code that receives such an outstanding evaluation? What we now refer to as the Napoleonic Code is the first of the five codes passed for France from 1804 to 1810 under Napoleon's rule (either as First Consul or Emperor). It contains much of the rules of the private civil law as it was considered expedient and practicable to embody in a single code. It consists of three books, preceded by a few preliminary articles on laws in general. Each book is divided into titles, each title into chapters, and each chapter into articles (Ilbert, 1905, p.5). The Code is often said to embody new ideas that emerged during the Revolution: nationalism, secularism, and above all, individualism. "The Civil Code was in reality the child of the Revolution, like Napoleon himself," one historian notes (1905, p.5).

However, some scholars have taken the opposite position; the French Civil Code is not as revolutionary as many perceive. In the first part of this study, we will see that the Code only has limited relevance to the Revolution; some articles even contradict what the revolutionaries embraced. They reflect, in fact, the principles of French treatise writers from the *ancien régime*, many of which were extracted from passages from ancient Roman thinkers (Gordley, 1994, p.1). The second half of the study will discuss the Code's relevance to the contemporary world. We will see that despite its unparalleled significance, its influence on global jurisprudence gradually declined by the twentieth century, when its evident limitations proved incompatible with the changing society.

Relevance to the Revolution

France was long divided, almost equally, into two great legal regions: the region of written law, based on the Roman law of Theodosius and Justinian, and the region of customary law. The two distinctive legal systems were compatible to a certain extent with local diversities, yet the fact of their concurrence within a sovereign state proved chaotic. Attempts to unify law commenced under the reign of Charles VIII and Louis XII. Vigorous and instrumental efforts were made to digest the customary law, and by the late sixteenth century, the customs of all the provinces had been reduced to a written and authoritative form (Ilbert, 1905, p.5). By 1681, under the instructions of Louis XIV, Chancellor Colbert established the Grande ordonnance de la marine and extended it to the whole country. These laws were the "immediate predecessors of the Napoleonic Codes," (1905, p.5) as they suggested the form and supplied the materials of the latter. Thus, the Napoleonic Code was not a precedent in unifying French law. It was more of a product of reexamination and integration of sources from ancient times.

If we closely examine the process behind Napoleon's codification, we can identify its adherence to Roman ideas. The fundamental condition of Napoleon's creation was a longing for a stable social order – after a decade of unrest and radical transformations – that resembled the *pax romana*. He believed in the Roman conception that his will would be legitimately imposed on native and conquered peoples through a system of laws (Kelley, 2002, p.3). The product, or the Code itself, exemplifies the influence of Roman law – despite it, like Justinian's *Corpus Juris Civilis*, was claimed to make obsolete all "Roman laws, ordinances, local or general customs and regulations" (1865). In many aspects, Napoleon preserved the old principles. His endorsement of the concept of property, or "Romanoid paternal power," family integrity, and other bulwarks of the emerging bourgeois establishment all reflect his attachment to Roman precedents (Kelley, 2002, p.9). In practice, as Kelley concludes, rationality in French law was almost extensively achieved via "recourse to these same sources," and most importantly, Roman law, which was "identified with reason itself;" the so-called ratio scripta or raison écrite by jurists (2002, p.8).

The codification, then, seems rather to be a "natural expression of the genius of the French people," who had been engaged for centuries prior to the fall of the Bastille upon the genial task of making the law into an orderly shape (Amos, 1928, p.3). In the discussion of specific provisions in the Code, we will trace back to the sources that did influence the framers, instead of radical ideas that emerged from the Revolution.

Property

Many scholars cited Article 544 as a typical instance of the Code's enshrinement of individualistic ideas (Arnaud, 1969, p.180; Halpérin, 1992, p.95). The original text is as follows: *La propriété est le droit de jouir et disposer des choses de la manière la plus absolue, pourvu qu'on n'en fasse pas un usage prohibé par les lois ou par les règlements* (art. 544, 1804). It defines ownership as the right to enjoy and dispose of things in the most absolute manner, if they are not used in a way prohibited by statutes or regulations. To determine whether the clause incarnates the spirit of individualism, we must first understand the origins of the idea of private property. The earliest remarks on this topic were in two great works in history. One of such was Gratian's *Decretum*, when Saint Ambrose reprimanded the rich who failed to provide for the poor's needs: "Let no one call his own what is common" (Gratian, 1855; Gordley, 1994, p.5-6). Another reference was in Aristotle's *Politics*, a critique of his teacher Plato's theory that all property should be held in common. Aristotle argued that there will be "perpetual quarrels," and "those who labor much and get little will complain of those who labor little and get much" (Aristotle, 1905; Gordley, 1994, p.6). Thomas Aquinas summarized the arguments and concluded that private property is a human institution modifying natural law, to which Roman law subscribed, to eliminate the disadvantages that would arise if all things were held in common (Aquinas, 1963).

This vision, however, was not reflected in Article 544. The provision made no explicit reference to a modification of natural law ideas and embracing individualistic principles. It simply states the definition of property, which scarcely contains a trace of individualism. Contemporary French writers, as Gordley observes, have fallen into a tendency of glossing the word "absolute" to connect the codification to the glorious legacies of the Revolution. If we examine the drafting history and the early commentaries of the Code, we will realize that a new individualistic theory of property is missing (Toullier, 1828, p.41-46; Duranton, 1844, p.202-03). In fact, the drafters never broke with the idea in Roman law that all things should be held in common. When presenting his first and third drafts, Cambacérès explained that it was not his task to decide theoretical controversies about the origin of property (Gordley, 1994, p.8). In short, in terms of property, the framers of the Code did not express much attention to new liberal ideas that became popular during the Revolution. Instead, they tended to hold on to the old natural law that all goods should be held in common, which, to a certain extent, contradicts individualistic principles.

Contract

Another controversial provision regarding individualism relates to contract. Article 1134 states: *Les conventions légalement formées tiennent lieu de loi à ceux qui les ont faites. Elles ne peuvent être révoquées que de leur consentement mutuel, ou pour les causes que la loi autorise. Elles doivent être exécutées de bonne foi* (art. 1134, 1804). In other words, agreements lawfully entered into take the place of the law for those who have made them. They may be revoked only by mutual consent, or for causes authorized by law, and they must be performed in good faith. Many scholars considered the text a proclamation of the autonomy of the will and the freedom of contract as it exalted contract to the same level as law. Some went further and claimed that the drafters themselves discovered this principle (Weill & Terré, 1986, p.10, 103; Carbonnier, 1977, p.66; Halpérinn, 1992, p.279). Yet, just as we have discussed in the previous section, these writers tended to gloss over the original text with personal interpretations. If we focus on the passage itself, we can see that the reference to "autonomy" was obscure. The article does say agreements take the place of law. It does not, however, reveal anything about autonomy (Bürge, 1991, p.64-65). Hence, the claim that the drafters built the Code on the revolutionary idea of individualism is far-fetched. What possibly influenced this definition of contract was Thomas Aquinas's theory that when something was transferred from one person to another, either it was an act of commutative justice that required an equivalent or it was an act of liberality

(Gordley, 1994, p.13). Such an idea was neither individualistic nor revolutionary.

Admittedly, the Code did incorporate principles of the Revolution when it was drafted. This study will focus on two of those. The first was the revolutionary idea that all men are created equal. The drafters did consider it in the codification. The other was the triumph of republicanism, which led to the creation of, as Gordley puts it, "an ideal of what a code should be" (1994, p.27).

Equality among all citizens

By 1791, the *Assemblée nationale* had extended full civil rights to Protestants and Jews. There is no doubt that the framers were deeply aware of equality among persons. According to Portalis, the Code aimed to eliminate "all civil differences based on religious conviction or hereditary social status" (Portalis, an XII). The civil laws would be based on "respect for morality, national honor, a passion for public liberty, the maintenance of the sacred rights of property, and the need to recognize no other distinctions than those of virtue and talent" (Jaubert, an XII). Here Gordley raised an interesting point: to what extent did the drafters have to modify French law to make it conform to the great principles of the Revolution? In fact, the law did not have to be changed much because the privileged and the disadvantaged groups were already granted the same rights as everyone else. As framers of the Civil Code, all Cambacérès and Portalis had to do was to avoid reintroducing special privileges for nobles and disadvantages for Protestants or Jews (Gordley, 1994, p.35-36). Thus, we see that the influence of the Revolution on the Code was relatively limited in this respect.

Republicanism

In the republican vision, the science of politics is appropriately applied to creating a rationally designed government built on the grounds of a comprehensive legal system. Instead of being ideological, the government applies a scientific methodology to governance problems through the study of past experience and experimentation in governance (Adams, 1787). If we translate this idea into legal terms, it means that the country's Code should be clear and self-sufficient; its rules would describe simple, natural relationships based on reason (Gordley, 1994, 28). Cambacérès, the chief redactor of the codification, seemed to be a firm advocate of this republican ideal. In a speech delivered during the presentation of the third draft of the Code, he stated that the primary objective was "a collection of precepts where everyone could find the rules for his conduct in civil life... Where judges are not legislators, it is not sufficient to ensure the authority of law by justice; it is also necessary that the laws be so disposed to eliminate doubt by clarity and prevent exceptions by foresight" (Cambacérès, an IV; Gordley, 1994, p.28). Had the final draft followed his remarks, one could argue its relevance to the Revolution. But these principles were rejected by the framers themselves; his drafts were voted down. To his colleagues in the committee, Cambacérès's idea was too idealistic; it was almost impractical to achieve. Such Code was too complicated, they recorded, and "more simple and more philosophical conceptions were wanted" (*Discussion devant le conseil des cinq cents, Sur le troisième projet de Cambacérès*, an V). Hence, all attempts to establish a republican Code failed, and new efforts to revise the drafts ceased.

When Portalis was appointed to carry on the project, he made it clear that the final draft was not supposed to conform to the republican ideal. In a great state such as France, he argued, both agrarian and commercial, with so many different professions, the laws could not be as simple as in those of a poor society. Nor would the Code make the dangerous attempt "to govern all and to foresee all" (Portalis, an IX; Gordley, 1994, p.30). Portalis's draft ultimately became the Code that we now know. It hardly shows any feature in line with the republican ideal that triumphed during the Revolution.

As we see, the purpose of Napoleon's codification resembles that of ancient Roman emperors, and the ideas that the framers embraced were almost extensively extracted from precedent intellectuals, both domestic and international. Albeit the efforts to incorporate revolutionary ideals into the codification, the civil laws themselves were loosely connected to the Revolution. Therefore, the Code only shows limited relevance to the Revolution.

Relevance to the Modern World

Another controversial question is how relevant is the Napoleonic Code to the modern world. In terms of radical social changes that it instigated, the influence of the Code is unparalleled. Its promulgation fundamentally transformed and reshaped societies in the old world. Without much exaggeration to say, the Code was the paradigm for any state that desired to establish a modern legal system for almost a century.

In our discussion of the Revolution and the codification, we see that although the drafters endorsed the revolutionary idea of equality among persons, the extension of such an idea was not achieved via the promulgation of the Code. The codification did, however, introduce relatively egalitarian conceptions about family. Under the *ancien régime*, marriage belonged to the domain of the canon law, which was under the control of the clergy. Families had to conform to Catholic traditions and regulations when planning a marriage. With the advent of the Code, marriage became a civil contract. The family law reduced the power of the father and raised the position of the wife. Indissoluble marriages were abolished (Lobingier, 1918, p.13); divorce was now recognized as a legal right (Ilbert, 1905, p.6). These changes greatly shaped our perception of a modern family; they were genuinely unprecedented at the time.

Applications of the Code Abroad

The Code did not merely transform the daily life of French citizens; it also made significant progress on a nationwide scale. Many writers underscored the idea of "people's law." By Fisher's evaluation, a more remarkable distinction of the Code is that it "has diffused the knowledge of law" and "made it comparatively easy for the ordinary Frenchman to become acquainted with the leading principles which govern the law of his own country" (1906, pg. 161; Lobingier, 1918, p.19). The ascendancy of its clearness made the Code an inspiration for jurists worldwide.

Over the course of the nineteenth century, the codification movement extended far beyond France. As Napoleon's army galloped over Europe, neighboring states immediately adopted the Code. Belgium has preserved it ever since, and the Rhine provinces only ceased to be subject to it on the promulgation of the German Civil Code in 1900 (Lobingier, 1918, p.20). Even after his humiliating defeat at Waterloo, monarchs continued to imitate his codification. In 1820, Tsar Alexander I appointed a commission to establish a code for the kingdom of Poland on the model of the French Civil Code. The drafters extracted passages from the original text, several parts of which were promulgated as law (Amos, 1928, p.14). Had the codification's influence only spread within Europe, its significance would be sharply reduced when we examine it worldwide. But the Code, along with the legend of the person who bore its name, had reached continents that were foreign to Europeans as well. Egypt was the first country to prepare its civil code on the grounds of the French Code in Arabic. When Nubar Pasha secured the consent of the Powers to the institution of the International Courts, it was unanimously agreed that the only possible law with which to equip them was that of the French Code (1928, p.15). This legal system was preserved even after the British occupation, giving rise to a peculiar society where British officials were administering and teaching French law (1928, p.15). Egypt was not a special case. As an awakening power of the East, Japan eagerly sought to modernize itself along western lines. One of the first acts after the Meiji Restoration was to translate the Napoleonic Code and invite French jurists to supervise the administration of justice and organize legal education (1928, p.15). The product of such effort was the Civil Code of Japan, which bore much resemblance to the French Civil Code. Though apparent distinctions existed between these codes aforementioned as they adapted to local diversities, their core was built, without exception, on Napoleon's codification.

Declining Influence in the Modern World

The contributions of the Code are, indeed, not negligible; it would be such a fallacy to deny these impacts. But recognizing them does not address the question that was posted at the beginning of this section: how relevant, then, is the codification to the "modern" world? To answer that, we must distinguish the "modern" world from the world two hundred years ago, when immediate transformations attributed to the codification occured. In two centuries, societies underwent changes that were previously unheard-of and unthinkable. We will see that the Code's influence in the world diminished by the twentieth century,

when its limitations became evident and proved incompatible with the changing society. To illustrate the evolution of the Code's status, we will focus on its application in a specific region – Latin America.

According to Lobingier, the Code has made itself, to a great extent, "the code of all the Latin races" Lobingier, 1918, p.16). His observation was not an exaggeration devoid of evidence, at least throughout the nineteenth century. The long admiration of French culture and ideologies was no secret in Latin America, especially among the educated elite class. In the wake of achieving independence in the 1820s, intellectuals in each country immediately commenced the codification and prepared for the passage of the civil laws. Like Egypt and Japan, the jurists made substantial references to articles in the French Code. The Haitian Civil Code of 1825 and the Civil Code of Oaxaca, Mexico, appeared to be exact copies of the Napoleonic Code (Mirow, 2005, p.5). In many countries, the Constitution rendered legal protection to the position of the Civil Code as a body of law. For instance, Article 67 of the Argentine Constitution states that while Congress has the power to modify the Civil Code by repealing or amending any of its articles, it can only do so expressly (Amos, 1928, p.5). In other words, any law that does not explicitly proclaim to alter the Civil Code but proves incompatible therewith is considered to be of no effect (1928, p.5). No region of the world placed the Code in such a high position as Latin Americans did.

However, by the twentieth century, the extent of the Code's influence gradually declined. Latin American jurisprudence had undergone substantial independent changes that deviated from the ideas in Napoleon's codification. The ultimate result was an evident reduction of French characteristics in contemporary private law. The study will analyze two primary factors that contributed to this departure.

One reason deals with the effects of globalization. We place it first because very few studies underscored its influence as a separate driving force. The twentieth century saw waves of globalization, primarily led by corporations that sought to extend their influence by operating on an international scale. Cooperations extended beyond borders, which diminished the significance of states and thus domestic law. Mirow notes that modern "business and property related transactions typically provide governing rules by contract or choice of law provisions" (Mirow, 2005, p.10). Under such circumstances, the Civil Code, which served as the foundation of Latin American domestic law, had become increasingly irrelevant (2005, p.10). As another consequence of globalization, Latin America has conformed to the tendency of avoiding traditional tribunals. It has adopted systems of alternative dispute resolution by mediation or arbitration, especially when resolving private law disputes (2005, p.11). This situation further limited the importance of the Code.

The growth of case law is another factor. As the United States consolidated its presence in the Western Hemisphere after the Second World War, its influence on the Latin American legal system increased. Throughout the second half of the twentieth century, Latin Americans were exposed to Anglo-American law through American education (2005, p.9). As a result, case law, or judicial precedent, had exerted significant influence in Latin America, a region once exclusively under civil law jurisdiction. This transformation is exemplified by the development of tort law and constitutional law (Miller, 1985, p.611; Bartels & Madden, 2001, p.59; Mirow, 2005, p.12), which required judicial interpretations of constitutional provisions by the Court. It is not surprising to see this process happening in an increasing number of states. The Napoleonic Code, after all, is a product of the old world, a world before globalization and the United States' dominance. It contains limitations that are unforeseeable to the drafters but evident to us. When developments in the modern world –from the twentieth century – magnified these limitations, jurists began to abandon the Code, therefore diminishing its influence.

Reforms and Revisions of the Code

In fact, in France and many countries where the civil law was based on the French model, calls for revisions to – if not a complete abandonment of – the Code were never absent. Part of the reason was technical issues. When explaining the prevailing tendency of decodification, historians evaluated that the old structure of the Napoleonic Code is no longer a useful organizational device as a result of the complexity and volume of new legislation (Lira, 1998; Diez-Picazo, 1992, p.480-81). The number of areas requiring legislative action has greatly increased as societies experienced constant transformations.

This situation is present in all categories: labor law, agrarian law, mining law, and family law (Mirow, 2005, p.12). On many occasions, it seems too arduous to incorporate the new topics into the structures of the existing Code. For more than a century, French jurists had made efforts to insert laws enacted after the codification into the Code, but eventually they found themselves in a predicament: new articles were poorly drafted and often with scarcely any consideration of the harmony and the order of the Code (De La Morandière, 1948, p.7). Therefore, most of the newly-passed laws were separate from the old Code. It was, after all, an impossible task to be completed. The Code formed a sharp contrast with nascent foreign codes in the twentieth century, represented by the German Civil Code, which were much easier to use (1948, p.8).

Had technical difficulties been the sole issue, it would be reasonable to question the departure of states from the Code. However, not only was the structure of the codification obsolete, but also were the articles themselves. Some laws included were simply unsuitable in the context of the contemporary world. Many ideas expressed by the French framers proved incompatible with the values of modern society. To provide a few examples, in family law – although considered relatively modern at the time it was published – the Code strengthens parental authority (1948, p.9). Articles 213 to 217 explicitly state the husband's authority in the family and the virtue of being an obedient wife (art. 213-217, 1804). Moreover, as Brissaud observes, the codification was "preoccupied" by the conservation of the real property in the family despite the abolition of primogeniture and entail (1912, p.732; art. 215, 1804). Such beliefs expressed in the Code were abandoned and objected to in later views. For each article mentioned above, at least one revision, if not repeal, was made. Among others, the marriage clause was constantly modified. Restrictions for women on contracting a second marriage were modified two times prior to its repeal in 2004 (art. 228, 1804).

Likewise, laws regarding private properties also underwent significant changes. During the twentieth century, many states had departed from the traditional *laissez-faire* system and attempted to direct the market. The government intervention in the production and redistribution of wealth greatly contradicted the exercises of property rights (De La Morandière, 1948, p.10). It undermined the protection of private property that the drafters of the Code had envisioned. It is plain that a hundred years after its promulgation, Napoleon's codification became obsolete. In multiple aspects, it was outcompeted by codes that were newly promulgated. For states that were deeply influenced by French jurisprudence, the most practical solution was not a complex revision of the existing Code, but an adoption of a new Code that could better serve society. In this case, the diminution of the Code's significance is inevitable.

Conclusion

In short, this study breaks two common perceptions that many possess. Firstly, the French Civil Code does not demonstrate as great relevance to the Revolution as it purports to be because most ideas expressed by the framers were extracted from the works of writers before the nineteenth century. Secondly, the influence of the Code has been significantly reduced due to its incompatibility with modern society, both its structure and its contents. This is by no means to question its contributions to the world. There remains no doubt that the codification placed a role with unparalleled importance in the development of global jurisprudence. What we challenged in this study were the myths of the Code, and we observed a tendency of overemphasizing the legacy of the codification.

Acknowledgements

I would like to thank Dr. Carlos Hernandez and Ms. María José Giubi for their feedback and for guiding me through the research and writing process.

References

1. Adams, J. (1787). *A Defense of the Constitutions of Government of the United States of America*.

2. Amos, M. (1928). The Code Napoléon and the Modern World. *Journal of Comparative Legislation and International Law*, 10(4), 222-236. Retrieved from https://www.jstor.org/stable/753418

3. Aquinas, T. (1963). *Summa theologica* (3rd ed.). Biblioteca de Autores Cristianos.

4. *Aristotle*. (1905). Aristotle's Politics. Oxford: Clarendon Press.

5. Arnaud, A.-J. (1969). *Les origines doctrinales du Code civil français*. Strasbourg: FeniXX réédition numérique.

6. Bartels, N. M., & Madden, M. S. (2001, Spring). A Comparative Analysis of United States and Colombian Tort Law: Duty, Breach, and Damages. *Pace International Law Review*, 13(1), 60-92. Retrieved from https://digitalcommons.pace.edu/cgi/viewcontent.cgi?article=1204&context=pilr

7. Brissaud, J. (1912). *History of French Private Law*. Translated by Rapelje Howell. Boston: Little, Brown, and Co.

8. Bürge, A. (1991). Das französische Privatrecht im 19. *Jahrhundert zwischen Tradition und Pandektenwissenschaft, Liberalismus und Etatismus*. Frankfurt am Main: V. Klostermann.

9. Cambacérès, J.-J.-R. (an IV, messidor). *Discours préliminaire prononcé par Cambacérès, au Conseil des cinq cents, lors de la présentation du troisième Projet de Code civil*.

10. Carbonnier, J. (1977). *Droit civil* (11th ed., Vol. I). Paris: Presses universitaires de France.

11. Code civil (1804). https://www.legifrance.gouv.fr/codes/article_lc/LEGIARTI000006428859/

12. De La Morandière, L. J. (1948, November). The Reform of the French Civil Code. Translated by Kurt H. Nadelmann. *University of Pennsylvania Law Review*, 97(1), 1-21. Retrieved from https://www.jstor.org/stable/3309648.

13. De Montholon, C. T. (1847). *Récits de la captivité de l'empereur Napoléon à Sainte-Hélène*. Paris: Paulin.

14. Diez-Picazo, L. (1992). Codificación, descodificación y recodificación. *Anuario de Derecho Civil*, 471-484. Retreived from https://revistas.pucp.edu.pe/index.php/themis/article/view/11054/11566

15. *Discussion devant le conseil des cinq cents, sur le troisième projet de Cambacérès*. (an V, pluviôse 9).

16. Duranton, A. (1844). *Cours de droit français suivant le Code civil* (3rd ed.). Paris: G. Thorel Libraire; Paris: Guilbert Libraire.

17. Fisher, H. A. L. (1906). The Codes. *The Cambridge Modern History* (Vol. IX). Cambridge: Cambridge University Press.

18. Gordley, J. (1994, Summer). Myths of the French Civil Code. *The American Journal of Comparative Law*, 42(3), 459-505. Retrieved from https://www.jstor.org/stable/840698

19. Gratianus, active 1151 (the Canonist). (1855). *Decretum Gratiani, emendatum et notationibus illustratum Gregorii XIII Pont*. Max. Paris: J.-P. Migne.

20. Halpérin, J.-L. (1992). *L'impossible code civil*. Paris: Presses universitaires de France.

21. Ilbert, C. (1905). The Centenary of the French Civil Code. *Journal of the Society of Comparative Legislation*, 6(2), 218-231. Retrieved from https://www.jstor.org/stable/752037

22. Jaubert, F. (an XII, ventôse 30). *Discours prononcé devant le Corps législatif*.

23. Justinian. (1865). *Corpus juris civilis. Leipzig*: Baumgaetner.

24. Kelley, D. R. (2002, Summer). Napoleonic Code and Roman Law. *History of Political Thought*, 23(2), 288-302. Retrieved from https://www.jstor.org/stable/26219837

25. Lira, B. B. (1998). *Estudios de derecho y cultura de abogados en Chile 1758-1998: tras la huella ius commune, la codificación y la descodificación en el Nuevo Mundo*. Scientific Electronic Library Online (Chile). Retrieved from https://www.scielo.cl/scielo.php?script=sci_arttext&pid=S0716-54551998000200003

26. Lobingier, C. (1918, December). Napoleon and His Code. *Harvard Law Review*, 32(2), 114-134. Retrieved from https://www.jstor.org/stable/1327640.

27. Miller, J. A. (1985). Products Liability in Argentina. *The American Journal of Comparative Law*, 33(4), 611-636. Retrieved from https://www.jstor.org/stable/840452.

28. Mirow, M. C. (2005). The Code Napoléon: Buried but Ruling in Latin America. *Denver Journal of International Law and Policy*, 33(2), 179-194. Retreived from https://ecollections.law.fiu.edu/cgi/viewcontent.cgi?article=1115&context=faculty_publications.

29. Portalis, J.-E.-M. (an IX, pluviôse). *Discours préliminaire prononcé lors de la présentation du projet de la Commission du gouvernement*.

30. Portalis, J.-E.-M. (an XII, ventôse 28). *Présentation et exposé des motifs devant le Corps-Législatif*.

31. Toullier, C. B. M. (1828). *Le Droit civil français suivant l'ordre du Code* (4th ed., Vol. III). Paris: Imprimerie de J. M. Vatar.

32. Weill, A., & Terré, F. (1986). *Droit civil: les obligations* (4th ed.). Paris: Dalloz.